Response to referees comments for *"Investigating the discrepancy between wet-suspension and dry-dispersion derived ice nucleation efficiency of mineral particles"* by C. Emersic *et al.*

We thank the referees for their insightful comment. Here we reproduce them in black, followed by our response in red. In the main text of the manuscript any changes have also been highlighted. A highlighted / tracked changed manuscript is appended to the end of the response.

Anonymous referee # 1

Major comments

1) Hiranuma et al. ACPD, 2014, stated "Though the number of immersed particles can vary from droplet to droplet and the random placement of particles in the drop may be of an effect on the ns values, the ns spectra from suspension measurements are in general in reasonable agreement even over a wide range of wt% of illite NX samples. Thus, the influence of the random placement of particles in the drop and agglomeration on the n_s estimation for suspension measurements seems small." This statement seems contradictory to the coagulation calculations in the current manuscript and conclusions reached in the current document. Please discuss.

We have investigated the effect of random placement of particles within drops in detail and did consider including this work in the current manuscript; there are differences when one considers the random placement vs bulk averaged placement of particles; however, we did not feel they were significant enough to explain the observations.

Here we reproduce some of our calculations on the random placement of particles to show the effect it has and argue that it does not explain the observed results.

We modelled the cumulative freezing curve one would expect in microlitre drops (Figure 1) and pico-litre drops (Figure 2) based on both bulk assumptions (which do not consider the statistical effects) and also statistical sampling, which considered the sizes of mineral particles one would expect in the drops and also the number of active sites one would expect on each of the mineral particles inside a drop. In the calculation one active site had to be present inside the drop, at a given temperature, for it to freeze. From this analysis we can plot out the theoretical cumulative freezing curve.

Looking at this analysis for micro litre drops (Figure 1) we see good agreement between bulk sampling and statistical sampling for both 0.8 wt% and 0.01 wt %; however, there is a slight difference at the highest frozen fractions, with the bulk method overestimating the frozen fraction at a given temperature slightly. This underestimation would result in an underestimation of n_s as calculated from the

experiments, because the experiment would measure lower frozen fractions than expected from bulk arguments alone. However, it is a minor effect.

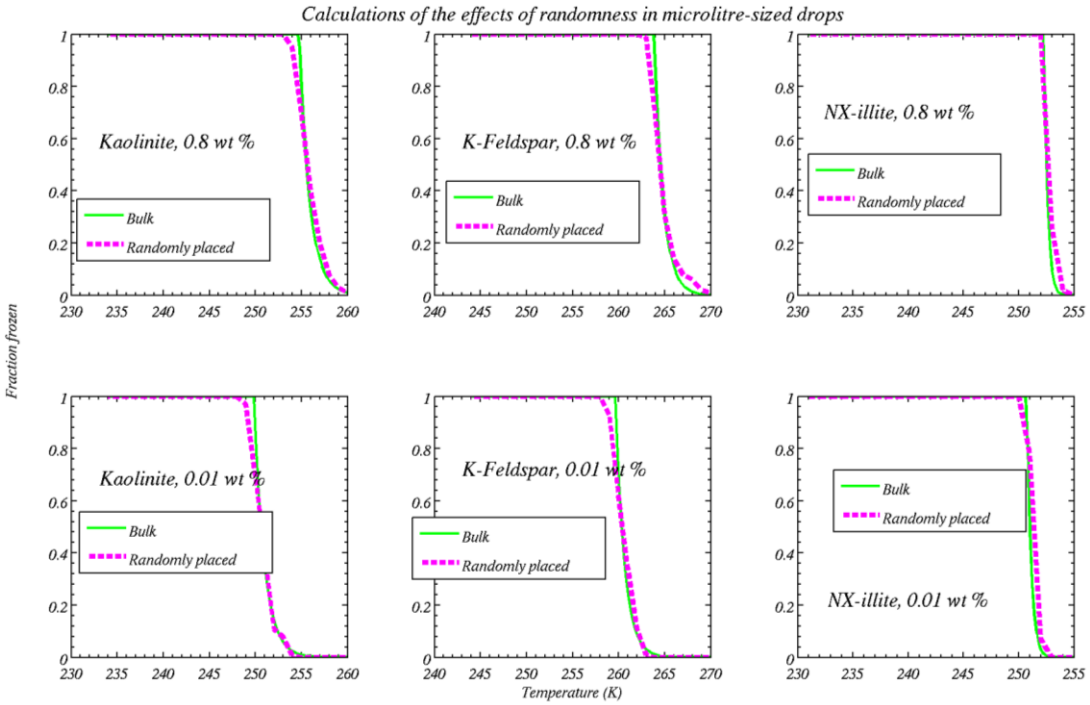

Figure 1. Modelled cumulative freezing curves in micro litre drops for Kaolinite, K-Feldspar and NX-illite. Green solid lines assume bulk averages for particle placement within drops and dashed magenta lines the random placement of particles within the drops. Top plots are for 0.8 wt% and bottom for 0.01 wt%. In general the agreement is very good; however, there are some small differences at the high frozen fractions, where the bulk consideration overestimates the frozen fraction.

In pico litre drops (Figure 2) this story changes slightly.The high wt % results (0.8 wt%) still show good agreement between bulk and random sampling; however, the low wt % (0.01 wt %) results show poorer agreement with not all drops freezing over the temperature range, in stark contrast to the bulk assumption. This is because it is possible to sample some drops that do not contain any mineral particles.

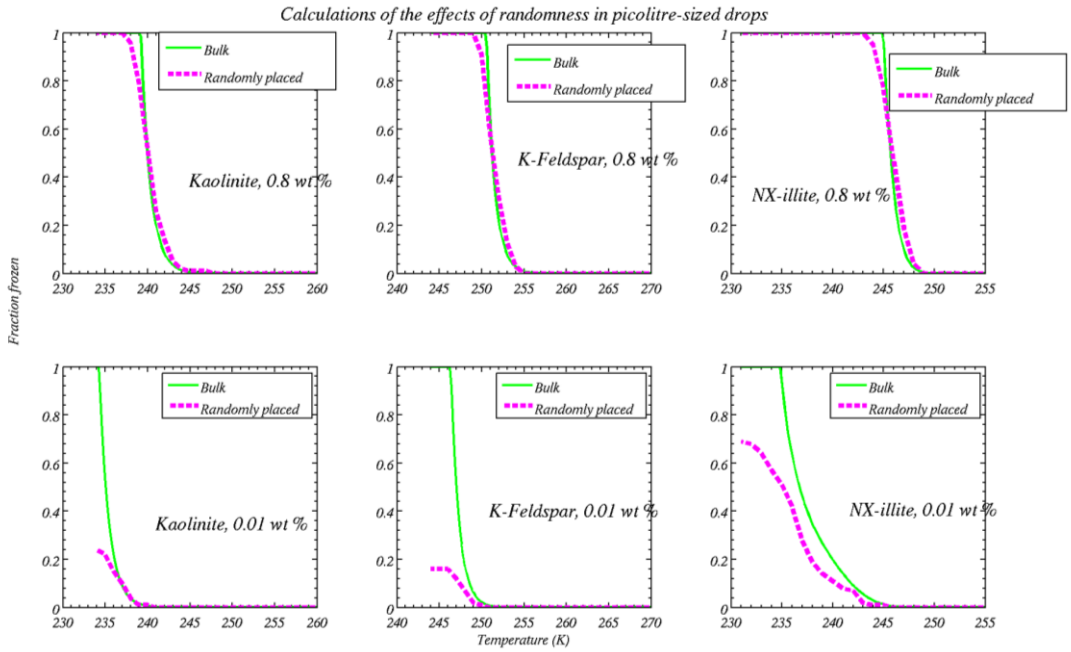

Figure 2. Modelled cumulative freezing curves in pico-litre drops for Kaolinite, K-Feldspar and NX-illite. Green solid lines assume bulk averages for particle placement within drops and dashed magenta lines the random placement of particles within the drops. The agreement is very good for wt % =0.8 (upper plots); however, the frozen fraction is significantly overestimated in the low wt % experiments (bottom plots). It should be noted that homogeneous freezing has not been calculated in these plots.

While this is interesting it likely does not affect our conclusions for two reasons:

- Only 0.8 wt % data are presented for the pico litre drops in Atkinson et al. (2013) on K-feldspar, so we have only compared with that data.
- The Kaolinite and NX-illite results for low wt % in pico litre will be masked by homogeneous freezing. That is homogeneous nucleation will freeze the drops anyway for temperatures less than about 238 K.

2) Were microliter samples with high concentrations of minerals used in the wet suspension experiments reported by Hiranuma et al. at temperatures of -28 C to -34 C?

The results presented in Hiranuma et al. for wet suspensions only go to temperatures as low as -24C so no they were not.

If microliter samples and high concentrations of minerals were used at these temperatures in the experiments reported by Hiranuma et al., then coagulation seems like an unlikely explanation for the difference between the dry dispersion and wet suspension experiments. Please discuss.

See above point.

3) It was not clear how the authors determined the ice particle concentrations reported in Table 1. For K-Feldspar at -21C the authors indicated with a footnote that

the CDP was used. For clarity, please indicate that CDP >18 microns was used (assuming this is correct). Also, does this mean the ice numbers from the 3V-CPI were used in all other cases or were 3V-CPI > 35 used in some of the other cases?

Yes thanks for pointing this out: we have made this clear in the revised manuscript.

4) In the text it was not clear how the authors determined the number of ice particles in the experiments and in some cases the decision sounded subjective. In some cases it sounded like they relied on ice particle concentrations from the 3V-CPI, but in other cases it sounded like they didn't rely on this result because the ice particles were somewhat rounded due to a lack of vapor growth. What criteria did they use to decide when to use and when not to use the ice measurements from the 3V-CPI. In addition in some cases it sounded like they used the data from the 3V-CPI > 35 microns to determine ice particle concentrations while in other cases it sounded like they did not since the 3V-CPI often over-sizes out of focus images of droplets (Connolly et al., 2007). What criteria did they use to decide when to use and when not to use the results from the 3V-CPI > 35 to determine ice particle concentrations? From my reading of this document it sounds like the results from the ice 3V-CPI should be used as a lower limit to the ice particle concentrations and the 3V-CPI > 35 microns should be used as an upper limit to the ice particle concentrations. Is this a valid statement?

It is correct that CPI is a lower estimate. The ice crystal concentrations determined from it are generally good when the sizes are greater than 40 microns. This is the case except at the lower temperatures when K-feldspar was used. Generally speaking when the particles are larger than around 40 microns we classify the images using automated software to discriminate ice crystals. When they are smaller it is more subjective, but we can be confident of a lower limit.

5) What is the uncertainty in the ice crystal concentrations determined for use in Equation 2? In table 1 the authors report an uncertainty from Poisson counting statistics, but what is the uncertainty from under counting with the 3V-CPI due to a lack of vapour growth and rounded ice particles and what is the uncertainty from over-sizing out of focus images of droplets with the 3V-CPI > 35 microns?

It depends on the size distribution. When particles are greater than around 40 microns we are fairly confident in the habit classification algorithm. If we are not sure, we have an unclassified category rather than risk erroneously classifying them as ice crystals. Because we are confident the remaining errors are due to Poisson counting errors.

6) In Figures 8 and 9 the authors should include the uncertainty in their results from the uncertainty in determining the ice crystal concentrations in their experiments (i.e. uncertainty from under counting with the 3V-CPI due to a lack of vapor growth and uncertainty from over-sizing out of focus images of droplets with the 3V-CPI > 35 microns).

Oversizing is not a problem for ice crystal classification. It is merely when the particles get large enough so that the classification algorithm works. We have made this clear in our manuscript.

Also, in Figure 9, have the authors included uncertainties in the parameterizations from Murray et al. 2011 (assuming uncertainties were given in the manuscript by Murray et al. 2011).

No, such errors were not included in the Murray et al (2011) manuscript.

7) Page 892, line 13-15, “However, the droplets lasted for a brief period (less than < 40 s).” Here the authors are referring to Figure 3, but in Figure 3 the black solid line suggests that the liquid droplets persist for at least 300 seconds. Please explain and give some explanation on how to interpret the black solid line in the bottom panels of figures 2-7.

Good spot! These are not actually drops, but the total from the CDP (cloud droplet probe), which includes aerosol particles, drops and ice crystals. Even though it is a droplet probe the CDP actually counts aerosol particles and ice particles. This is an oversight on our part and we have updated the figures to reflect this.

8) Related to the comment above, on Page 893 the authors indicate that in Figure 5 the kaolinite particles nucleated ice in the absence of cloud droplets. I am not sure how the authors reach this conclusion since the presence of cloud droplets are indicated by the black solid line in the third panel of Figure 5.

See above. Our oversight and has been corrected.

9) In the dynamic light scattering experiments, why not do the experiments as a function of time to determine coagulation rates. This seems more relevant since coagulation rates would be more directly comparable with the coagulation calculations?

The investigation of coagulation vs time would be of high relevance to our study. However, within the time required for a single light scattering measurement, particles had already reached a stable diameter. To our knowledge, the only two ways to actually observe aggregation are:

- Either manually decrease the run time for single measurements: this has been tried and proved to produce results with too low signal to noise.
- Decrease the concentration of mineral particles: unfortunately, one would have to decrease the concentration to values lower than the technique can deal with. Under these conditions the instrument struggles to scale the correlation function properly, preventing the correct measurements of particle size.

Note that over much longer time scales (t > 15 minutes) we often observed sedimentation of the particles and no measurements could be performed under these conditions.

10) It would be helpful to list the point of zero charge for the different surfaces of kaolinite.

We looked into doing this, but there are a range of values measured in the literature, so left this out of the manuscript. Its between about pH 4 and 5.

11) Section 5.1.1 The discussion on colloidal forces in suspensions is useful and does suggest that it may be reasonable to neglect repulsive forces in the coagulation calculations. However, this section does not provide conclusive evidence that repulsive forces can be neglected. I also came to the same conclusion from Table 2.

We are not in a position to state this unequivocally, but are hoping to purchase an instrument that can measure this soon. The calculations are meant as a useful first step. If anything the calculations may over estimate the coagulation rates, but what we aimed to show is that it is not inconceivable that aggregation is playing an important role.

That said when one uses the ion concentrations presented in Hiranuma et al. for illite in water (their figure 3) we find that the forces between two particles become attractive over a much wider range of parameter space than our Figure 13 suggests (see Figure 3). At the ion concentrations shown in Hiranuma et al. one also finds that the zeta potentials of the clay minerals is close to ~10 (mV) see Du et al. (2010) for an example, hence, Brownian coagulation is a reasonable assumption.

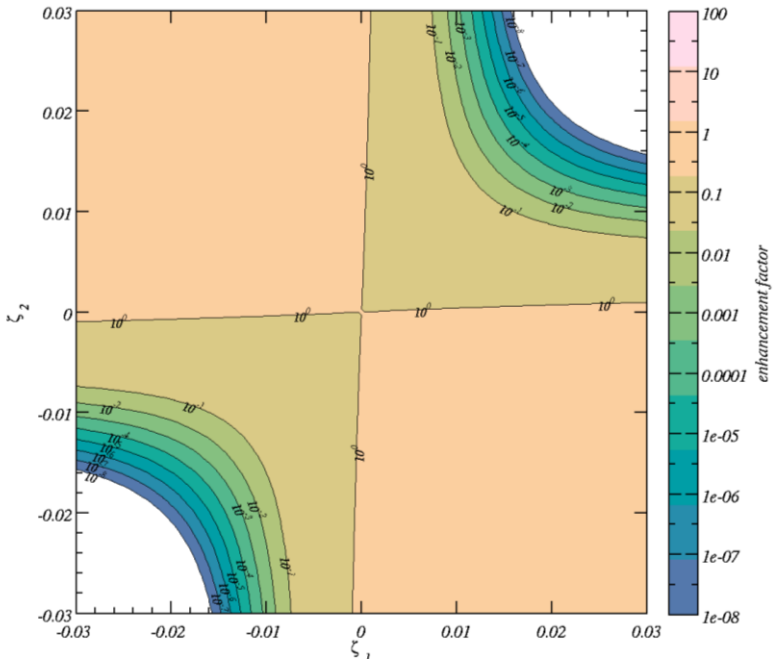

Figure 3. Enhancement over Brownian capture for two 0.1 radius micron particles with zeta potentials given on the x and y axes. Units for x and y axes are volts. This shows that a wider range of zeta potentials can give rise to attractive forces between particles in comparison to the assumption of pure water.

It would be more convincing if the authors did a time dependent study using dynamic light scattering to show that the force of repulsion can be neglected

See above point about instrument limitations.

Minor comments:

1) Page 890, line 9-10, are there any particles > 5 nm in the filtered air.

None in the filtered air, but they are in the chamber air, see Figure 7 and Figure 8. We can not get them out of the background, but we have shown conclusively that they are not significant ice nuclei.

2) Figure 11 and 12. For the red solid lines there is a sudden drop at the earliest times, and then a straight line. Why is this line not an exponential curve? Please comment.

It is, but it very quickly gets limited due to lack of particles. i.e. the concentration is high, but the total number is too low for aggregation to continue and the particle concentration to drop exponentially.

3) In Figure 2, consider changing “droplets” in the annotation to “droplets (CDP)” to be consistent with the other annotations

Thanks. It needs to be changed to total from CDP anyhow, as noted above.

4) Figure 2. Please indicate that the dashed blue line corresponds to the right axis.

You are correct and we have made this clear.

5) It may be helpful to include a short description on each of the instruments used to measure droplet concentrations and ice crystal concentrations (i.e. PALAS WELAS 2000, CDP, SPEC 3V-CPI) since they are crucial to the interpretation of the data.

We have done this.

6) The figure caption indicates CDP > 20 microns, but the text refers to CDP > 18 microns. These two numbers should be the same to avoid confusion

Good spot, thanks and we have changed this.

Anonymous referee #2

Major comments

The main concern for referee #2 was whether aggregation of the mineral particles could happen within droplets on a cold stage.

We don't see why it would not happen if the concentrations were high enough – why should it be significantly different to the bulk? That said following discussions we believe that aggregation is an important effect in all drop sizes, but most likely happens in the bulk suspension. Aggregation apparently happens in pico-litre drops in the clay minerals except at low concentrations, but it is not particularly evident in the Feldspar experiments. We believe this is due to the morphological differences between clays (platelets, which are more likely to bond strongly) and Feldspars. The Feldspars are more likely to form weaker aggregates in suspension, which may be disrupted when introduced into drops and aggregation may only be possible in the micro-litre drops as discussed in our manuscript.

They argue that statistical fluctuations of mineral particles within the drops is potentially a larger effect and cite Wright and Petters

We have looked at this somewhat too, with a numerical simulation (see our reply to the first comment of referee #1), but did not find it to be a significant effect, especially in microlitre drops. See Figure 1 and Figure 2.

They suggest the following sentences are too bold for the evidence presented:

-P888, L10-12 ", revealed the…"

-P888 L18-21 "revealed that…"

-P899 L22-26

-P902 L1-8

-P905 L8-10

There is the suggestion to tweak the structure to have section 4 separated into subsections.

We currently feel that some of these methods belong in the results because they are part of the investigation. It is not a huge task to put into the methodology and if there is a good reason for it we may be convinced otherwise, but it is our preference to leave them here.

Minor comments

P 888 L6 & L 13: I suggest maintaining consistency of terms with a previous publication. The correct notation should be either ice-active surface site density

(IASSD; Connolly et al., 2009) or ice nucleation active surface-site density (INAS density; Niemand et al., 2012). The same applies elsewhere, e.g., P889 L 13 & L 16, P 894 L12.

We have done this.

P889 L5-6: Hiranuma et al. discusses the potential effect of agglomerates and multiple nucleation modes besides chemical aging effect.

Correct, this is now stated.

P889 L11: Consider giving the description of Kaolinite (e.g., KGa-1b from Clay Mineral Society) here instead of Sect. 5.

done.

P894 L3-4: So the surface area is scaled to the droplet number to calculate ns? If so, it is worth mentioning for clarity.

done

P896 L8: Awkward sentence. I suggest rephrasing.

done

P896 L15-16: The curves were manually fitted to the data.

We think you are suggesting we omit the phrase, “but fitted the data very well”. We have done this.

P896 L19: Two lognormal modes according to Table 1?

Yes, good spot.

P897 L1: 1-5% in mass? surface area?

In mass, it is now stated.

P897 L26: This sentence seems incomplete - do not to well what?

Should say “do not do well”. Changed now.

P898 L2: wet-suspension according to its first appearance.

Good, thanks.

P899 L7: between to?

Should be “two”

P900 L3 : I suggest using wt% to be consistent with what appears in figures. The same goes to other parts, e.g., P900 L 23.

Good, thanks.

P900 L4: M Ω cm

Yes.

Dr Benjamin Murray's comments

General comments

Emersic et al. present a paper in which they compare chamber derived ns values with parameterisations from the literature based on droplet freezing experiments. They present results for K-feldspar, kaolinite KGa-1b and nx-illite. The dust samples for these investigations were supplied by the authors of this comment as part of a collaboration between the groups at Manchester and Leeds in order to facilitate an inter-comparison of techniques.

At lower temperatures for each dataset they find good agreement between their chamber and the literature droplet freezing experiments, but at higher temperatures they report a larger ns value for the chamber measurements. They go on to offer an explanation for this discrepancy.

While we are in agreement that a thorough inter-comparison of different methods to evaluate INP efficiencies is an important issue for the community, we do not see how this paper constructively adds to the effort and we do not recommend publication in ACP in its current form. In terms of the general topic, the **discrepancy between many ice nucleation instruments has already been reported and discussed** by Hiranuma et al. (2014) in a much more comprehensive inter-comparison article. The new and novel part of the paper is the discussion of aggregation in droplet freezing experiments.

The article mentioned above, Hiranuma et al. (2014) is more comprehensive from the point of view of more techniques were inter compared; however, it only investigated one sample, namely illite-NX, so from another perspective it is not as comprehensive; hence, we believe our results are an addition to current knowledge and note that this is stated by referees #1 and #2. In Hiranuma et al. aggregation was flagged as an important topic for further investigation in the full article, which is now published in ACP. Our paper validates the MICC results by comparing the illite-NX results with the previous literature (in our Figure 8) and adds more information on two extra mineral powders.

However, Emersic et al.'s explanation for smaller ns values from droplet freezing experiments relies on the unsubstantiated assumption that aggregation of particulates substantially reduces the surface area of dust available for nucleation or that aggregated particles somehow fall out of the droplets. The authors have not taken into account a **significant body of literature which shows that coagulation does not substantially reduce the surface area of mineral dust** and that there is no dependency of ns on mineral dust concentration.

The question of whether flocculated mineral particles offer less surface area than deflocculated mineral powders is a valid question to ask. Nevertheless regardless of whether flocculated minerals offer less surface area it should be recognised that

once colloidal particles reach sizes of 2-5 microns, which is what we are suggesting can happens, settling times are of the order of less than 20 minutes. Thus it is still possible to reduce the surface area available for nucleation. Aggregated platelets are shown from SEM images of the kaolinite sample (Figure 4) that has been in suspension and subsequently dried out. We see evidence of very large stacks of platelets and argue that there is the potential for a reduction in the surface area available.

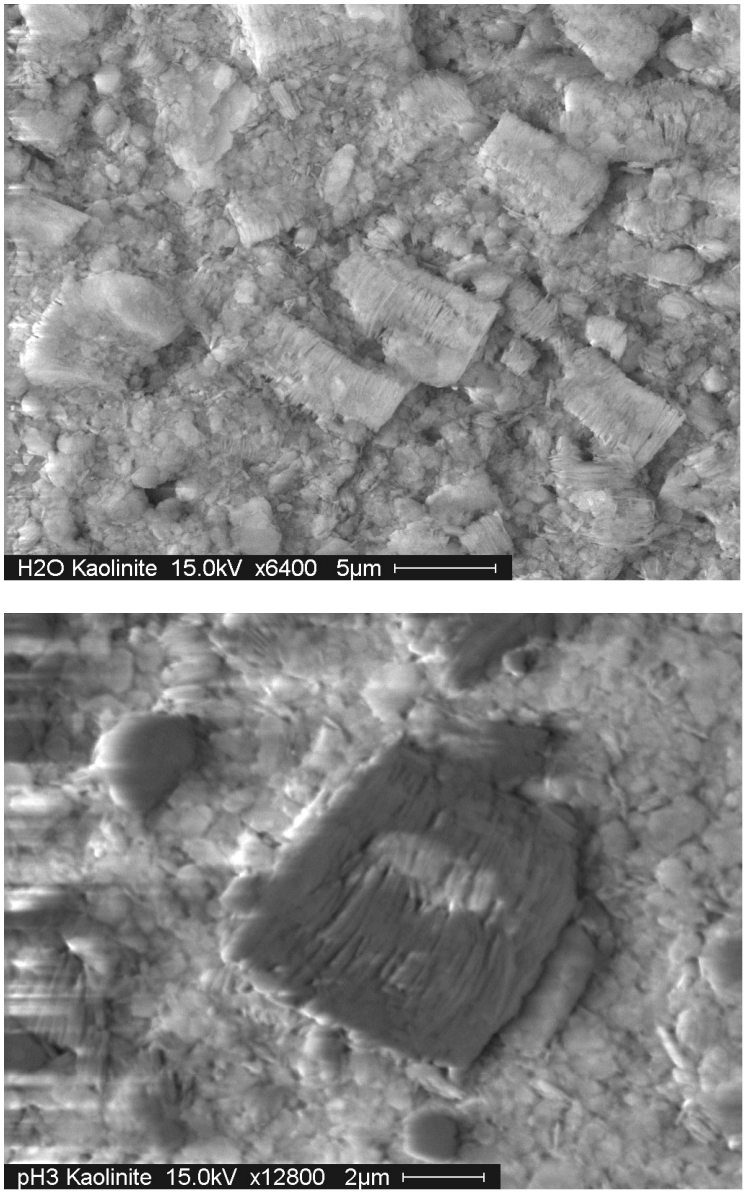

Figure 4. SEM images of aggregated kaolinite particles that have been in suspension.

We are not aware of any “significant body of literature” that specifically shows that coagulation does not reduce the surface area available for nucleation and would be grateful to be directed to this literature.

Additionally, the authors have not compared their results against all of the available data from experiments with the same materials. Comparison with literature data

shows that the Manchester ice cloud chamber data is inconsistent with other dry-dispersed instruments such as continuous flow diffusion chambers.

It is true that data from the Manchester chamber are slightly higher than some of the CFDC counters. CFDC counters also suffer from artefacts and many of the scientists who work with them are trying to understand these very useful instruments. One issue is that, even when operated at supersaturated conditions, the CFDC counters do not guarantee that the 100% of the sample activate into drops. This is relevant because we are considering immersion / condensation freezing in our paper. A specific sentence from the published literature where this is stated is actually in the Hiranuma intercomparison paper (that Benjamin Murray co-authored) just before section 3.3. Here it is very clearly stated that, ***"the lower ns of CSU-CFDC may be a consequence of the underestimation of Nice, possibly due to its constrained RHw (at 105%) and the disturbance of aerosol laminar between two plates in a CFDC (DeMott et al. 2015)."***

An important aspect of the results we present here is that the slopes of the n_s vs temperature curves are consistent with those for natural dusts (e.g. those shown in Niemand et al. 2012) whereas those from wet-suspension (Murray et al. 2011; Broadley et al. 2012; Atkinson et al 2013) tend to be much steeper. This is illustrated in the recent publication by Atkinson et al. (2013) where a comparison is made between observed and modelled ice nuclei concentrations using curves derived from wet suspension experiments for the modelled ice nuclei.

We have reproduced data from Atkinson et al. (2013, figure 4 f) and added an assessment based on the Niemand curve (that our data are consistent with) in Figure 5, essentially rescaling the Atkinson et al. figure 4 f by the ratio of the Niemand curve to the scaled Feldspar line.

Admittedly there are many uncertainties in such an analysis, but we note that there is arguably better 1 : 1 agreement between model and observations if the Niemand curve is used instead of the wet-suspension data. Figure 5 thus shows that when data are adjusted to n_s curves that have a slope that is closer to those of natural dust (and our data) that agreement is better between observations and model.

Thus we consider that the wet suspension technique may be underestimating n_s by some means to be a strong possibility. We looked at several aspects of the problem, including the distribution of particles within the suspension (see Figure 1 and Figure 2) and arrived at the conclusion that aggregation may be an important loss of particle surface area.

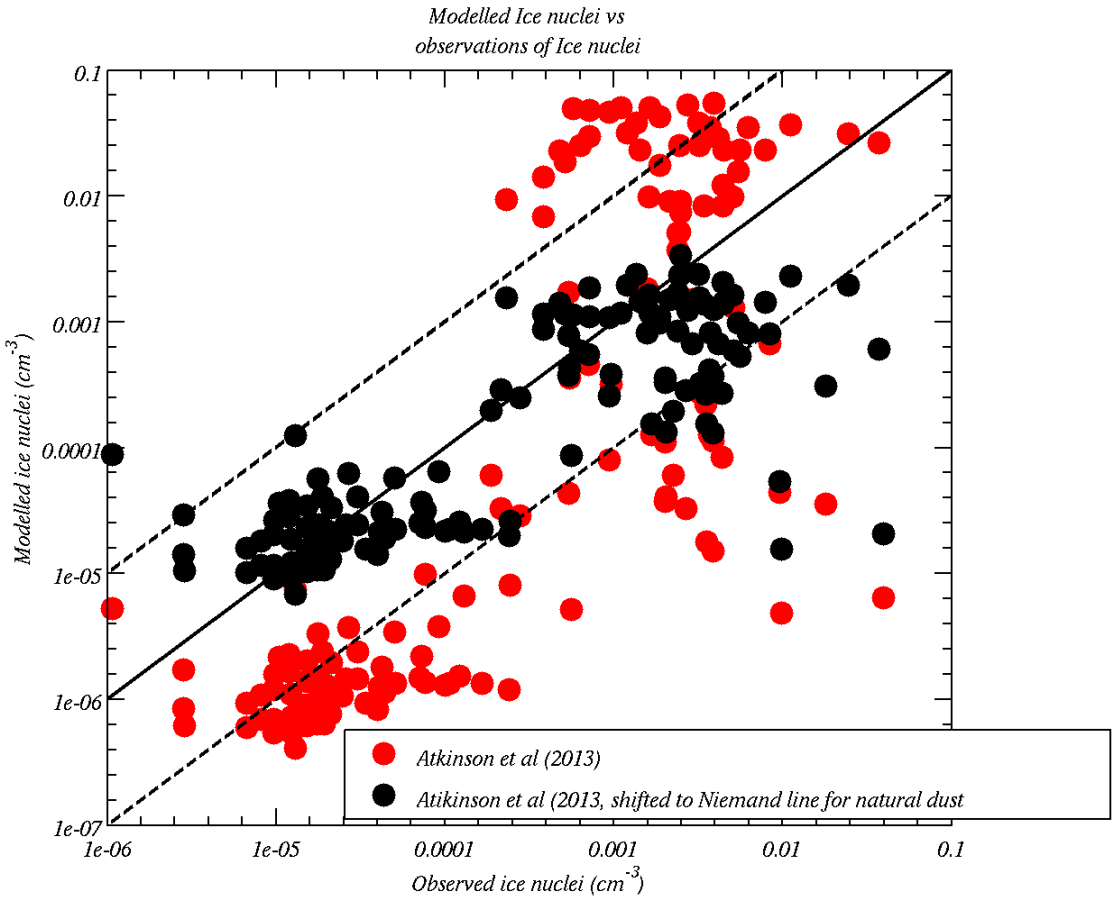

Figure 5. Data reproduced from Atkinson et al. (2013, figure 4f) red lines as well as the same data shifted to the Niemand curve, which has a slope that is consistent with the data presented in our article.

In fact, the wet-dispersed droplet freezing experiments are consistent with a number of data sets with dry-dispersed dusts. This brings into question the basis on which the paper is founded. Emersic et al. claim to be motivated by the 'discrepancy between wet-suspended and dry-dispersed derived ice nucleation' efficiencies (as stated very boldly in the title).

our response above addresses this statement. The title of our manuscript picks up on the current status of the literature and specifically the paper on Hiranuma paper on illite-NX, where it is stated that:

"the ice nucleation activity expressed in ns was smaller for the average of the wet suspended samples and higher for the average of the dry-dispersed aerosol samples between about -27C and -18C"

But, there is not a clear cut discrepancy between dry-dispersed and wet-suspended particles and the reference to Hiranuma et al. (2014) has been taken out of context. We reproduce the key plots from Hiranuma et al. to illustrate that there are

discrepancies between different instruments rather than a simple divide between dry-dispersed and wet-dispersed instruments

Benjamin's comment above is referring to the fact that some CFDC techniques also do not agree. This point was raised above and our response is that the Hiranuma et al paper clearly states ***"the lower ns of CSU-CFDC may be a consequence of the underestimation of Nice, possibly due to its constrained RHw (at 105%) and the disturbance of aerosol laminar between two plates in a CFDC (DeMott et al. 2015)."***

Specific comments

1. Emersic et al. make the argument that coagulation of particles occurs when mineral dust particles are suspended in water and assume that this reduces the surface area available for nucleation by many orders of magnitude at high particle concentrations in microliter volume droplets. However, the evidence in the literature (discussed below) shows that surface area is not significantly reduced through coagulation

We contest that the data presented in the referees comment show that "surface area is not significantly reduced." The data presented by Benjamin Murray actually show that n_s values are consistent over a wide range of weight percents when microlitre droplets are used. We believe that aggregation can occur in the wet suspensions over a wide range of concentrations. Several details also depend on sample preparation, for instance, if a stock suspension is made up and then diluted this can also lead to aggregation at the time when the high concentrations are present in the suspension.

Putting these difficulties aside we have performed some model simulations that show that the aggregation effect is high, but relatively insensitive to wt % over the regime 0.05< wt % <2.0 as shown in Figure 6. We discuss this in more detail in response to a similar point made below.

and cannot account for the differences between the ns datasets.

See above.

It is already very well known that mineral dust particles tend to form aggregates. The vast majority of particulates in both dry dispersed and wet-suspended experiments are already aggregates of smaller particles. I include an image of a typical dry particle of nx-illite in which we can see that it is made up of many aggregated individual grains of just a few 10s of nanometres in size. This is prior to any aggregation in suspension and is representative of the particles used by Emersic et al. in their chamber.

We agree there is some degree of aggregation in the dry samples; however, we argue that the aggregation is amplified in the wet suspension. See Figure 4, which shows SEM images of kaolinite particles that have been in suspension and then dried out. The layered nature of the particles is evident and one can see that this particular particle has aggregated face-to-face many times.

So, is the total surface area of wet suspended particles strongly influenced by aggregation? Here we present multiple lines of evidence which show that there is not a strong effect and that most of the 'internal' surface area of an aggregate remains available for ice nucleation.

i. The authors correctly state that aggregation becomes more important for higher particle concentrations in suspension, but their claim that this will substantially reduce the surface area available for nucleation is unsubstantiated. Aggregation leading to loss of surface area is something which has been tested within the remit of the INUIT intercomparison (Hiranuma et al., 2014).

They state on page 22 that "agglomeration may conceivably affect the surface area exposed to liquid water" and in section 4.4 "Further quantification…is an important topic for future works".

Wet suspended experiments were performed with several droplet freezing instruments each using droplets containing a range of nx-illite concentrations. For example, in BINARY (instrument based in Bielefeld) the surface area was varied by a factor of 100, in NIPI (the Leeds instrument) it was varied by a **factor of 10** and in the North Carolina instrument it was varied by 4 orders of magnitude. The resulting ns values are all self-consistent within a single system which shows that there is no impact on ns values by particle aggregation.

The interesting point here is that within this range of wt% in micro litre drops the modelled area fractions are not that sensitive to the initial wt%. Figure 6 below shows coagulation calculations over the course of a day for wt %=0.05, 1.0 and 2.0. Here it is shown that the surface area of particles divided by initial surface area tends towards similar values in all three simulations.

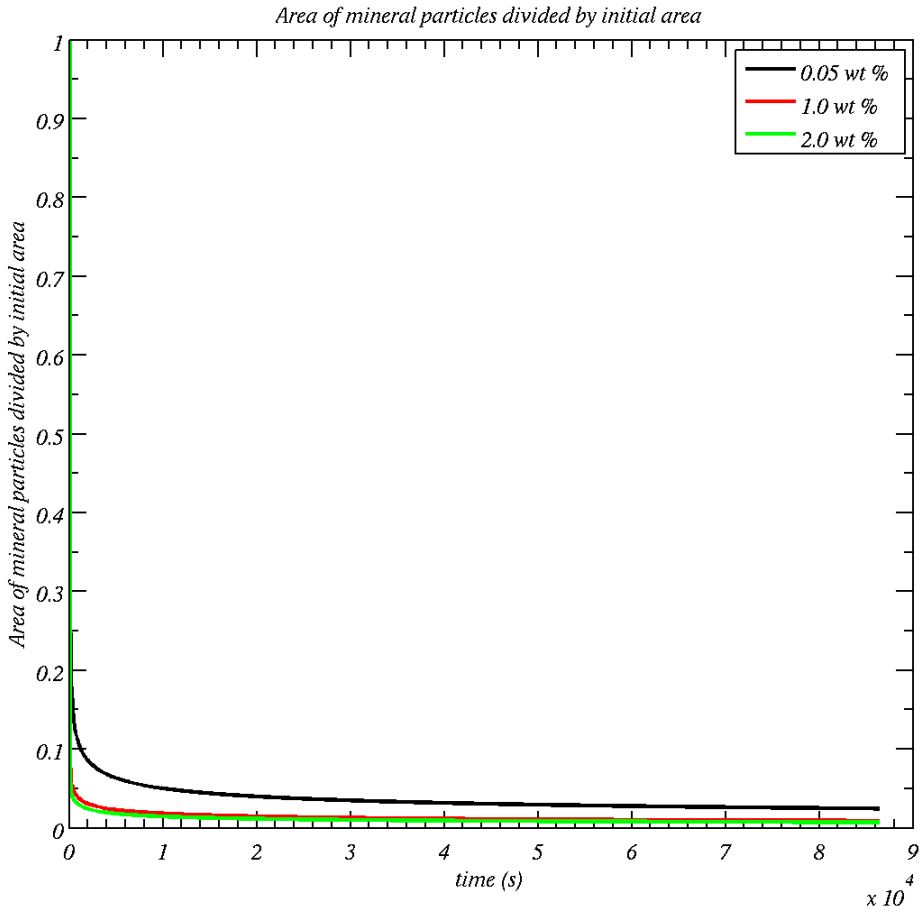

Figure 6. Sensitivity of aggregation to wt % in the range 0.05< wt % < 2.0

A caveat in these calculations is that you should not trust them to be 100% accurate, but only to an order of magnitude because there are several uncertain parameters in the calculations. For instance the zeta potential is very important to determining how effectively the particles are able to come together and stick, but its value is quite uncertain. Another area of uncertainty is in how the particles aggregate together (ie. do they form quasi-spheres or to form stacked plates?): it is not clear how they should aggregate from first principles but either assumption will lead to different results. In addition to this we have not taken into account enhancement of the coagulation kernel by shear motion in the fluid. Nevertheless the picture that emerges from this first cut treatment is that the surface area ratio is relatively insensitive to particle number.

This is all assuming the wt% does not affect the zeta potential of the mineral particle, but in actual fact the wt% could slightly alter the zeta potential. Slight changes in zeta potential can make large differences to the coagulation kernel.

To reinforce this view we have plotted new data from NIPI for nx-illite in microliter volume droplets in Figure 2. The dust concentration was varied from 0.05 to 2 wt%. The values of ns from the experiments with widely varying dust concentrations overlap, hence ns is independent of dust concentration and therefore independent of aggregation.

To be explicit, we do not believe this offers evidence that aggregation is not affecting all of the results presented (see Figure 6 above, which shows the fractional area left over after aggregation is relatively insensitive to wt % in this regime, but that it is very much lower than the initial value).

ii. The individual mineral dust grains which make up a mineral dust aggregates are irregular and stack in an irregular manner leaving space between the grains for gas or liquid, i.e. aggregation only has a minor impact on total surface area.

In our opinion this argument is invalid. The very fact that they "stack" can lead to a large difference in surface area (see Figure 4 for instance). A more quantitative counterargument is needed to rule it out in our opinion.

This view is borne out by both gas adsorption measurements and methylene blue adsorption on particulates in aqueous suspension. Broadley et al. (2012) showed that the BET gas adsorption surface area implied a primary particle size for nx-illite of 10s nm. This was consistent with electron microscope images where aggregates of 100s-1000s nm in size were composed of many smaller primary grains of 10s nm in size (Figure 1).

The soil science community also uses a method to quantify surface area of clay minerals suspended in water (Hang and Brindley, 1970). This technique involves placing a known quantity of methylene blue in an aqueous suspension and recording how much adsorbs onto the clay mineral from which they determine the surface area. They show that the BET and methylene blue specific surface areas are consistent which unambiguously shows that the internal surfaces of aggregates are accessible to molecules much larger than water such as methylene blue

The paper by Hang and Brindley uses a much lower wt% than those under consideration here. For example, at the bottom of page 204 of the Hang and Brindley article (left column) they say they use 5 mg in 200 ml of water, which is 2.5×10^{-3} wt%.

In addition in the technique described by Hang and Brindley (end of page 204) they start with mineral particles dispersed in methylene blue solutions and observe that the absorption of methylene blue increases with time. They do observe flocculation of the clays (as stated on page 204), and they consider a plot of methylene blue concentration vs amount absorbed. They argue that where the gradient of this curve starts to drop off is the point that defines the specific surface area, because the particles are flocculating. Central to this assumption is that there is only one

monolayer of methylene blue on the mineral particles at this point, which is not a given.

Another point is that the BET vs MB surface areas reported in the Table of Hang and Brindley only agree to within a factor of two. Hence, the agreement is more order of magnitude OK, rather than exactly the same.

2. Emersic et al. also suggest that coagulation 'removes the particles from the drops by sedimentation'. The mechanism through which the authors envisage micron scales particles to pass across the air-water interface through the side of a droplet is not discussed. But, the fact that aggregation is expected to be mineral dust concentration dependent and that we observe no dependence of ns over a wide range of mineral dust concentrations (discussed in 1i) shows this is not a major loss of surface area.

We think this is a misinterpretation. We are suggesting that the particles sediment in the bulk suspensions…but they can still aggregate within the drops. We have made this clear.

3. Potential problems with measuring ns at the Manchester Ice Cloud Chamber (MICC). This paper represents the first ever published measurement of ice nucleation efficiency in the MICC chamber. Despite the many issues which could affect the results from a complex instrument and the subsequent analysis of the data the resulting ns values are regarded as 'truth'. Rather than validating their own instrument and results, they focus on why other instruments might be wrong.

They need to show that their instrument is capable of making these measurements.

We have compared our results to the AIDA published data for NX-illite and they agree – see figure 8 in our manuscript. This is good validation of our experiment.

Here are some selected issues that we think should be clarified:

i. Background measurements are mentioned, but are not shown. Is a measurement of 2 ice crystals per cm3 really significantly above the background? The background runs need to be performed with all the possible artefact aerosol sources, such as mixing fans, valves, inlet pipes, etc, used with clean filtered gas. ii. What has been done to test for temperature gradients in the chamber? What standard experiments have been done? Can MICC reproduce homogeneous freezing rates, for example?

Figure 7 shows a background experiment at -12 to -20C. You see the activation of cloud drops on the CDP (middle plot) by the presence of a closed drop mode and the lack of ice is indicated by two pieces of evidence: (1) in the middle plot the lack of particles outside of that mode; (2) in the bottom plot by the lack of ice on the 3V-CPI.

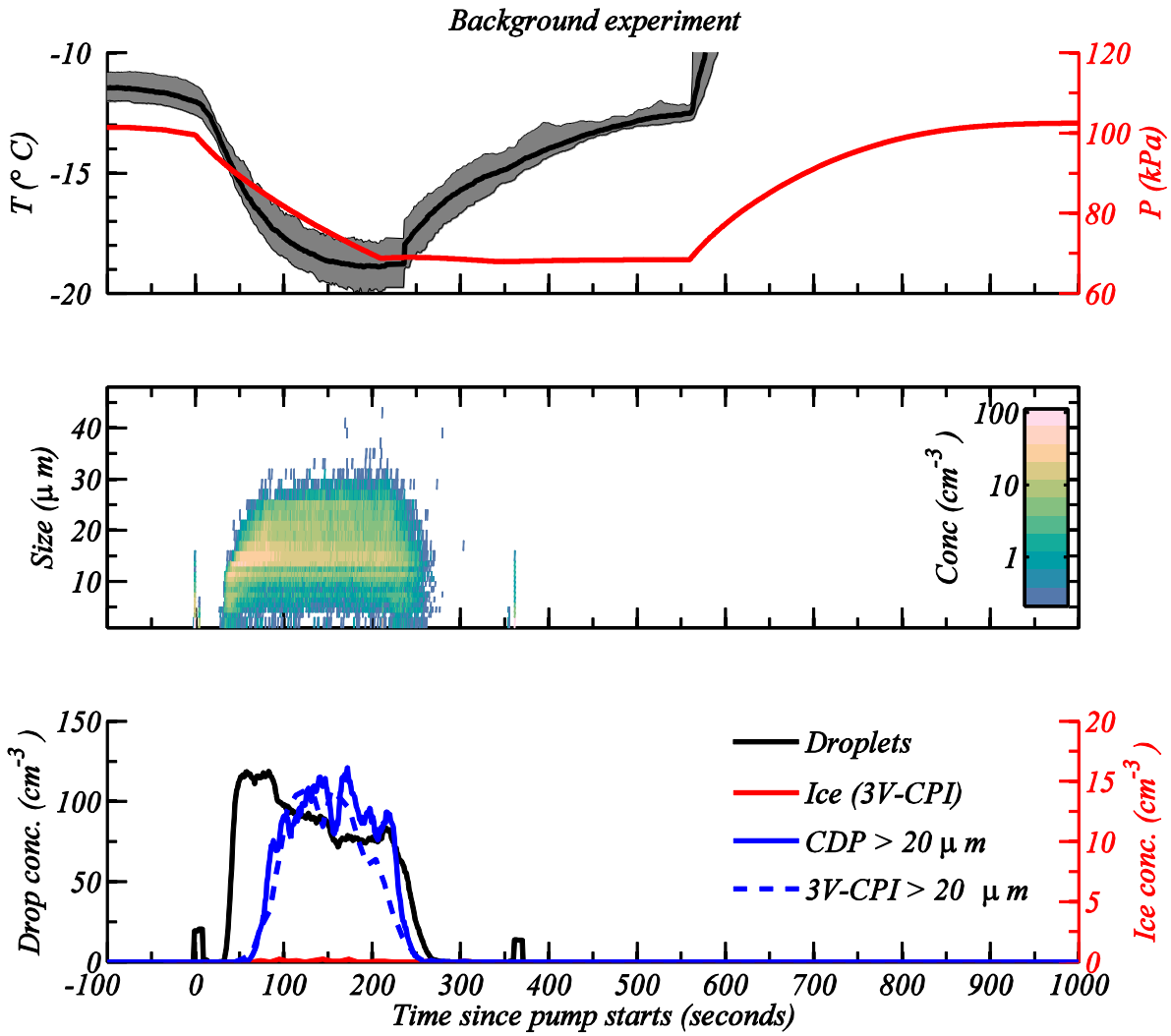

Figure 7. Background experiment at -12 to -20C.

Figure 8 shows a background experiment at -20 to -28C, the same point is true although here the background ice concentration is slightly higher (about <0.2 /cc). Ignore the spike at the end of the run – this is due to electromagnetic interference when the valves close. We have also done this at -25C, but there we get to temperatures as low as -33 - -34C and see evidence of homogeneous nucleation at the end. We have not done the analysis to see if this reproduces homogeneous freezing nucleation rates because that is a separate problem.

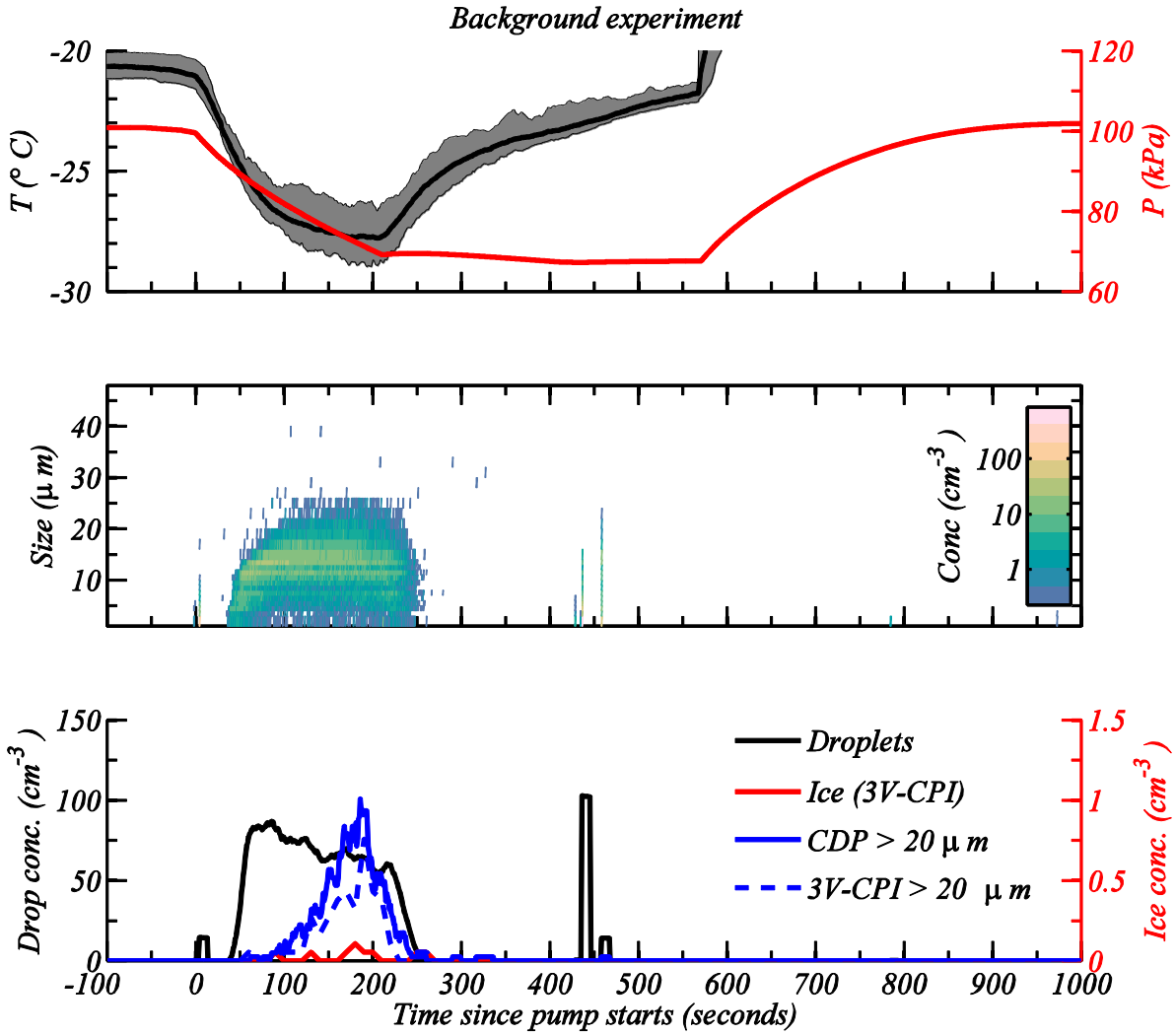

Figure 8. Background experiment at -20 to -28C.

iii. The geometry of the chamber is quite different from chambers which are focused on cloud nucleation research. The MICC chamber is 10 m tall and just 1 m wide in contrast to the AIDA chamber which is 7 m tall and 4 m wide. The geometry of the AIDA chamber minimises interaction of the cloud with the walls. The MICC chamber is described by Emersic et al. as a fall tube and has only been used in the past for ice aggregation work (at least this is the only published work from the chamber: Connolly et al. ACP. 2012).

In addition to the aggregation work, the chamber has also been used to study a wide variety of problems including:

Kaye, P. H., Hirst, E., Greenaway, R. S., Ulanowski, Z., Hesse, E., DeMott, P. J., Connolly, P. J. (2008). Classifying atmospheric ice crystals by spatial light scattering. Optics Letters, 33(13), 1545–1547.

Ávila, E. E., Castellano, N. E., Saunders, C. P. R., Bürgesser, R. E., & Aguirre Varela, G. G. (2009). Initial stages of the riming process on ice crystals, DOI: 10.1029/2009GL037723

Smith, H. R., Connolly, P. J., Baran, A. J., Hesse, E., Smedley, A. R. D., & Webb, A. R. (2015). Cloud chamber laboratory investigations into scattering properties of hollow ice particles. Journal of Quantitative Spectroscopy and Radiative Transfer, 157, 106–118. doi:10.1016/j.jqsrt.2015.02.015

The instrumentation to detect droplets and ice is all located at the base of the chamber, up to 10 m away from the region in which nucleation could occur. Are artefacts introduced by having to rely on sedimentation of crystals out of the main volume of the chamber to the detectors?

No because we do not rely on sedimentation. We sample air from the chamber, so actively suck the air out. In addition are data agree well with AIDA for illite-NX as shown in our Figure 8.

How homogeneous is temperature? Cold spots 3-4 K colder in the warmer temperature experiments might explain the discrepancies in ns.

Temperatures are slightly inhomogeneous – it is not as well mixed as AIDA, but the temperature difference measured at 8 separate locations is less that 1K as can be seen by the margin of error values in the time series of temperature in Figs 2-7 (which show the full range rather than standard deviation values).

iv. What is the background INP concentration with the rotating brush generator running with just gas flowing through? This is a rather vigorous way of making aerosol and I worry that flakes of metal and previous dusts make it into the chamber. When measuring just 2 ice crystals in 2000 dust grains minor impurities will become problematic.

See Figure 7 and Figure 8 on the background issues. Additionally, the rotating brush generator was completely dismantled and vigorously washed clean of any powder then dried each time we changed the mineral powder under investigation. This yielded a good background (see above).

v. What are the error bars on the measurements in figure 8? There seems to be a very large spread in estimated ns values. For example, the nx-illite data around -21oC varies by 2 orders of magnitude. Is this within the experimental uncertainty or does it indicate that there is some other uncontrolled dependency which is not addressed.

No, this is just removal of the most effective IN during several repeat experiments. The difference is a factor of about 30, which is attributed to the most effective IN being used up. In the Hiranuma paper only the first expansions were shown, so we have made this clear now.

This could be something like a dust preparation dependency.

We don’t believe this is the case, due to the argument above.

4. Emersic et al. have focused their comparison plot (their fig 8) on the data from my team and show just the dry-dispersed and wet-dispersed average data from Hiranuma et al. (2014). This is odd because there now exists a wealth of literature data using the exact materials used here which the authors could also compare their results to (see below). It is our opinion that the omission of the literature data from this comparison is a major error and has led Emersic et al. to make incorrect claims. We suggest that data for each material is plotted on a separate plot together with the pertinent literature data.

Below I explore how the new Emersic et al. data compares with literature data:

i. Nx-illite. There is a wealth of information available in the Hiranuma et al. (2014) intercomparison paper where many of the world's ice nucleation research teams used their respective instruments (17 in total) to quantify ice nucleation with the same material. This dataset cannot be simply summarised in two lines – the dry-dispersed and wet-dispersed lines in Emersic et al.'s Fig 8. I have reproduced the data set in Figure 3 and have added the Emersic et al. data to Figure 4 in which the data are split into dry-dispersed and wet-suspended. The discussion in the Hiranuma et al. paper is far more subtle and caveated than Emersic et al. suggest (and has also been modified in the accepted ACP article; they cite only the ACPD version). If you take a simple average of the two groups of data, you apparently get wet suspended lower than the dry dispersed ns. But, taking a closer look it is clear that the CFDC, a dry-dispersed technique that cannot be susceptible to aggregation effects described by Emersic et al., are consistent with the wet-suspended experiments.

This comment about the CFDCs is addressed in an earlier comment above.

The Manchester data is inconsistent with the CFDC data from ETH (PINC) and Colorado State (Instrument name?). Discussion of why the new Emersic et al. data is inconsistent with the CFDC data needs to be included in the paper.

We will address the concerns over the discrepancy with CFDCs as stated above: in short the literature clearly state that the CFDCs may underestimate n_s (see Hiranuma et al. prior to section 3.3).

ii. Kaolinite KGa-1b. Again, Emersic et al. have ignored most of the literature data.

Tobo et al. (2014) summarise some kaolinite results together with recent literature data for KGa-1b in their Fig A1. This figure is reproduced here together with the Emersic et al. data superimposed (Figure 5). There is a mixed picture here. The dry-dispersed CFDC data from Tobo et al. (2014) and the dry dispersed Wex et al. (2014) data are in good agreement with the wet-dispersed Murray et al. (2011) data, but the Kanji et al. (2013) data also from a CFDC, is somewhat higher. The new Emersic et al. data sits between these two extremes, but is more than one order of magnitude greater than the Murray et al. (2011), Tobo et al. (2014) and Wex et al.

(2014) data. This does not support the premise that there is a strong difference between dry dispersed and wet-suspended experiments.

We reproduce Benjamin Murray's plot below. There are several things to point out:

- First of all, our data at low temperatures has been omitted. This data, at around -32C, agrees with all of the data except the Kanji (2013) results.
- Secondly, we address the comparison to the other instruments at warmer temperatures, where our results are higher than the others.
    - The results from Schill et al are using wet suspensions and may also suffer from the problems we are discussing.
    - The results from Tobo et al are fitted to data from a CFDC (see above argument)
    - The results cited as being from Wex et al. are also a fit to the same CFDC data as Tobo et al. because the original article says that measurements with LACIS were made at temperatures -30, -34 and -38C (see page 5536) and the other measurements were with the CSU CFDC.
    - The operator of the CSU CFDC admits that there may be an issue in activating all particles to drops (in the Hiranuma paper)

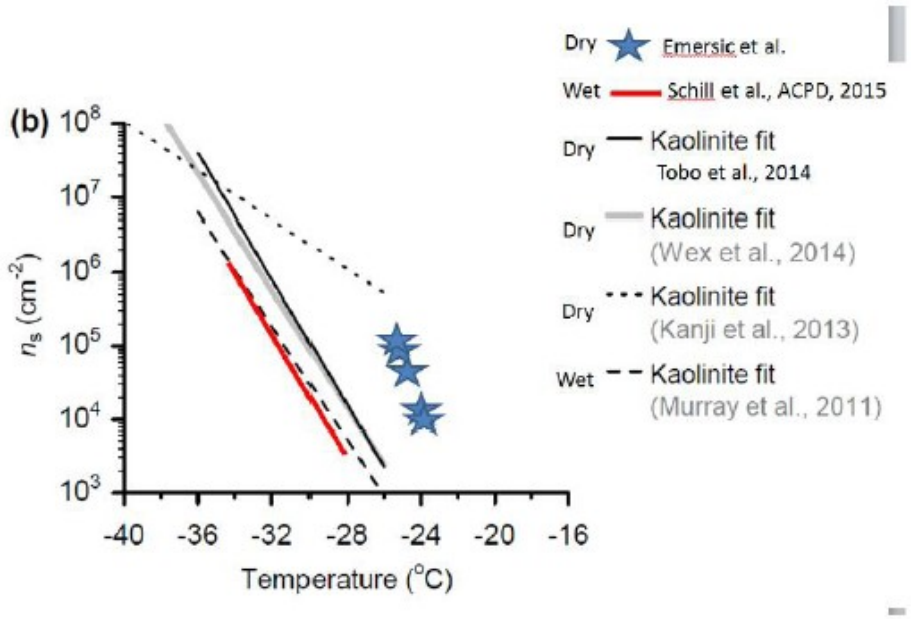

Figure 1. Figure comparing data for Kaolinite KGa-1b adapted from Tobo et al. (2014) with the addition of the Emersic et al. data and that of Schill et al. (2015). The dry dispersed results of Wex et al. (2014) and Tobo et al. (2014) are in good agreement with the wet dispersed data of Murray et al. (2011) and Schill et al. (2015). The results of Kanji et al. (2013) are somewhat higher above about -34°C. The data of Emersic et al. are inconsistent with all data sets and substantially higher than two of the dry-dispersed datasets which is inconsistent with their aggregation hypothesis.

5. Emersic et al. have extrapolated the fits presented in Murray et al. (2011), Broadley et al. (2012) and **Atkinson et al. (2013)** well beyond the regime where measurements were made and the stated validity range of those parameterisations. They then use these extrapolations to claim that there is a difference between the chamber and droplet freezing approaches. This is not valid. The nx-illite ns polynomial parameterisation (Broadley et al. (2012)) extends up to -25 C, whereas Emersic et al. quote data around -21oC. In Broadley et al. (2012) we made it very clear that extrapolation would be incorrect, stating: 'since this parameterisation is based on experimental data with surface areas 2x10-6 cm2 it may under predict ice nucleation above 247 K. Similarly, for Kaolinite we only quote data up to -27oC, whereas Emersic et al. assume in their argument that there is a discrepancy on experiments at warmer temperatures. The fits in Fig 8 need to be limited to the range where measurements were made and the discussion modified accordingly.

The measurements from Broadley are superseded by the INUIT measurements in any case. The conclusion is the same regardless. We dispute that we have extrapolated results from Atkinson et al. (2013): the K-feldspar curve from Atkinson et al. spans the range 247 K to 270 K (see their Figure 3) and our results span 247 to 255 K.

6. The ns data for from Murray et al. (2011) and Broadley et al. (2012), plotted in their Fig 8, is based on droplets with diameters of 10's micrometers. These droplets are closer to picolitre in volume rather than microliter. Emersic et al. suggest that it is the microliter volume droplets where there is an aggregation problem. Given the Murray et al. (2011) and Broadley et al. (2012) data is not based on microliter experiments they should not suffer from aggregation issues according to the analysis of Emersic et al. Hence, aggregation cannot account for the differences between the chamber and these droplet freezing studies.

We are not saying it is not an issue for the pico litre-sized drops. We are saying that it probably does not happen within the drops when they are pico litre sized, but it could still happen in the bulk suspension. Whether or not it does will depend on sample preparation. Whether or not the particles stay in an aggregated state when making the drops will depend on whether clays or feldspars are under consideration. Clays tend to form strong aggregates because of they are platelets, whereas feldspars form looser aggregates.

7. The authors claim that feldspar is not susceptible to coagulation and should therefore not be affected. However, their data is still more than one order of magnitude higher than the Atkinson et al. (2013) parameterisation at around -18oC. Doesn't this imply we need to look for a different explanation other than aggregation?

This is a misinterpretation, what we mean by that is that the Feldspar sample forms weaker aggregates because of their morphology. Hence, we are suggesting that the

Feldspar aggregates can be easily disrupted when introduced into pico-litre sized drops.

8. Quoting from Emersic et al.: ‘Illite and kaolinite particles may behave differently and could coagulate during the stirring process.’ The authors suggest that aggregation of particles occurs during stirring. The action of stirring breaks up aggregates, not the other way around. This is the whole point of stirring – it breaks up aggregates to create a more stable suspension.

We disagree that stirring will always act to break up the aggregates. One only needs to consult the wide body of literature on this subject to learn that aggregation / flocculation can be greatly enhanced by shear within the fluid under certain conditions. These are text books that cover some of these details:

Jacobson, M. Z. (1999). ``Fundamentals of atmospheric modelling". ``Cambridge University Press".

Crowe, C. T. (2006). MULTIPHASE FLOW HANDBOOK. City, 1218, 6092–101. doi:10.1016/j.chroma.2011.01.063 (see page 6-11)

9. ‘Ben Murray’ in the acknowledgments: The draft which I saw was very different to this one and I should not be acknowledged for comments. We should be acknowledged for providing the samples as part of the ACID PRUF consortium.

We have made this change on your request.

Comment from Heike Wex

The main comment to address here is the statement that data from the LACIS chamber agrees with data from Benjamin Murray's group

We have reproduced the figure included in this communication and would like to point out that the red line starts to come away from the orange line at around T=-24C. This is completely consistent with our data for K-feldspar, but unfortunately the data do not extend far enough to lower temperatures. The error bar for NX-illite is too large to say much.

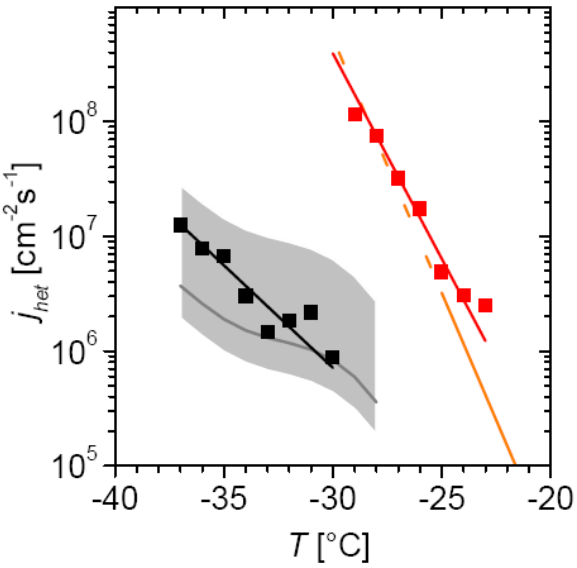

Figure S1 (from Augustin-Bauditz et al., GRL (2014), supplement): Calculated nucleation rate coefficients for K-feldspar and illite NX as function of temperature. Symbols in red (K-feldspar) and black (illite NX) show data obtained from LACIS, together with the respective fits (lines). The orange and grey lines represent data from Atkinson et al., Nature (2013) for K-feldspar and Broadley et al., ACP (2012) for illite NX, respectively. The grey shaded area represents the uncertainty in the conversion from surface areas based on BET to those based on the assumption of spherical particles.

Furthermore, although they are interesting, we do not wish to comment on the biological samples as it is not relevant to the present study.

Manuscript prepared for Atmos. Chem. Phys. Discuss.
with version 2014/09/16 7.15 Copernicus papers of the LaTeX class copernicus.cls.
Date: 31 May 2015

Investigating the discrepancy between wet-suspension and dry-dispersion derived ice nucleation efficiency of mineral particles

C. Emersic[1], P. J. Connolly[1], S. Boult[1], M. Campana[2], and Z. Li[2]

[1]School of Earth, Atmospheric and Environmental Sciences, The University of Manchester, UK
[2]School of Physics and Astronomy, The University of Manchester, UK

Correspondence to: P. J. Connolly (p.connolly@man.ac.uk)

Abstract

Cloud chamber investigations into ice nucleation by mineral particles were compared with results from cold stage droplet freezing experiments. Kaolinite, NX-illite, and K-feldspar were examined and K-feldspar was revealed to be the most ice active mineral particle sample, in agreement with recent cold stage studies. The ice nucleation efficiencies, as quantified using the ~~*ice active*~~ *ice-active surface site density* method, were found to be in agreement with previous studies for the lower temperatures; however, at higher temperatures the efficiency was consistently higher than those inferred from cold stage experiments. Numerical process modelling of cloud formation during the experiments, using the cold-stage-derived parameterisations to initiate the ice phase, revealed the cold-stage-derived parameterisations to consistently under predict the number of ice crystals relative to that observed. We suggest the reason for the underestimation of ice in the model is that the slope of the cold-stage-derived ~~*ice active*~~ *ice-active surface site density* vs temperature curves are too steep, which results in an underestimation of the number of ice crystals at higher temperatures during the expansion. These ice crystals suppress further freezing due to the Bergeron-Findeison process. Application of a coagulation model to the size distribution of mineral particles present in the suspensions as used in the cold-stage-derived parameterisations ~~revealed that it is likely~~ is used to investigate the idea that the mineral particles coagulate in suspension, which either removes the particles from the drops by sedimentation, whilst in the bulk suspension, or reduces the total particle surface area available for ice nucleation to take place. ~~This is confirmed with~~ Aggregation is confirmed using dynamic light scattering measurements of colloidal suspensions. The implication is that the mineral particles may be more important at nucleating ice than previously thought at high temperatures.

1 Introduction

Recently Hiranuma et al. (2014) determined ice nucleation efficiency of the NX-illite dust sample using a variety of methods. The methods were broadly classed as "wet-suspension" methods, where mineral particles were put into water suspension before droplets of the suspension were cooled and frozen, or "dry-dispersion" methods, where the mineral particles act as cloud condensation nuclei followed by freezing. Hiranuma et al. suggested that there was a discrepancy between the dry-dispersion methods and the wet-suspension methods at high temperatures, which they attributed to a change in chemical composition of the NX-illite mineral during dissolution in water. They also discussed the potential effect of agglomerates and posibility of multiple nucleation modes, and suggested that further work was needed to better understand instrumental limitations.

Atmospheric mineral dust particles are comprised of several different minerals (e.g. Glaccum and Prospero, 1980; Kandler et al., 2007) and it is possible to determine their ice nucleation activity (e.g. Connolly et al., 2009, and others). However, there is much to be learned by investigating the ice nucleating ability of less complex "pure minerals". Using a technique originally described by Vali (1971), Kaolinite (KGa-1b from the clay mineral society) and NX-illite have recently been examined in the immersion freezing nucleation mode (Murray et al., 2011; Broadley et al., 2012) and parameterisations of the ice-active surface site density have been put forward as have those for K-feldspar (Atkinson et al., 2013). These studies used "wet-suspensions" to investigate ice nucleation by immersion freezing. They quantified the ice nucleation ability of the pure minerals using the ice-active surface site density concept, described as the number of ice active sites per unit surface area of dust, n_s, as presented by Connolly et al. (2009).

Murray et al. (2011) showed that the number of ice active sites on dust scales with the total surface area of dust in a drop; however, the total surface area available in the droplets was relatively large due to high particle concentrations in the dust suspension used to generate the droplets. In some cases the number concentrations exceeded 10^{17} m^{-3}, which equates to an inter particle spacing of $\sim 2\,\mu$m, if one assumes equal spacing between the

particles. At these high particle concentrations one might expect some interaction between neighbouring particles if they are able to come together and adhere due to the van der Waals interaction.

In nature, it is unlikely such high dust concentrations will be present in supercooled cloud droplets. Hence, the aim of this paper is to use a combination of laboratory experiments, data analysis and modelling to reconcile two different approaches for determining ice nucleation efficiency.

2 Experimental set-up

Experiments were conducted in the Manchester Ice Cloud Chamber (MICC) fall tube, which has a diameter of 1 m and height of 10 m (additional details of the general facility are described in Connolly et al., 2012). The MICC and experimental set-up are shown in Fig. 1. Initially, the chamber was pressure sealed and evacuated using two scroll pumps, capable of reducing pressure at a rate of approximately 1.4 hPa s^{-1}, to 200 hPa before refilling with filtered air. The filtered air had 10–20 cm^{-3} < 5 nm particles, with a total particle mass concentration < 0.01 µg m^{-3}. Volatile Organic Carbon, VOC, measurements by the Leicester Proton Transfer Reaction Mass Spectrometer always indicated VOC levels below detection limits of approximately 1 ppb. This cleaning process was repeated a total of three times to reduce background aerosol concentration inside MICC to typically 20 cm^{-3}. The chamber was then cooled to the desired temperature, ranging from -12 to $-27\,^{\circ}C$ depending on the experiment, and allowed to thermally equilibriate.

Prior to conducting the cloud formation experiments, a background experiment was performed in which the pressure was reduced to 700 hPa to check that the remaining background aerosol in the chamber post-cleaning were not ice nuclei. Ice was only ever observed in low concentrations of a few cm^{-3} at the lowest temperatures and was attributed to homogeneous nucleation when the temperature during the pressure reduction process approached $-36\,^{\circ}C$. In the case where this was observed, the ice crystal concentration was

substantially lower than the resulting concentration in the later experiments where mineral dust particles were present.

Following the background experiment, a selected mineral dust was inserted into the chamber using a PALAS dust generator (RBG 1000 ID). This instrument uses particle free compressed air to separate and insert dust particles from a rotating brush which collects them from a reservoir. The dust was inserted into the top of the chamber and allowed to homogenise; an initial measurement was taken using an Ultra High Sensitivity Aerosol Spectrometer (UHSAS), which uses an intracavity laser to measure aerosols in the size range (50–1000 nm) and a PALAS WELAS 2000 aerosol probe indicating total initial concentrations of approximately 1000–2000 cm^{-3}.

Liquid cloud drops formed as the pressure was reduced to 700 hPa from ice saturated conditions, and this was sampled with cloud probes, including the PALAS WELAS 2000 (WELAS), Droplet Measurement Technologies ~~(DMT)~~ Cloud Droplet Probe (CDP), and the Stratton Park Engineering Company ~~(SPEC)~~ Cloud Particle Imager ~~(CPI)3V which includes a 2-D-Stereo (2-DS) probe.~~ 3V (3V-CPI). Briefly, the WELAS infers the size of particles from the intensity of the light they scatter at 90°. The CDP operates on a similar principle to the WELAS, but uses a solid state laser (658 nm) and detects light scattered by particles ($3 < D < 50\,\mu$m) in the forward direction (4-12°). The 3V-CPI takes images of particles ($20 < D < 2000\,\mu$m), that pass through the sample volume, using a pulsed infrared laser incident on a CCD array. 3V-CPI images that are greater than 35 μm in length are analysed for their shape to determine if they are ice crystals or not. For these large shapes we are confident in discriminating between drops and ice crystals; hence, the remaining errors are due to Poisson counting.

Internal chamber pressure was measured using a Lex 1 Keller pressure probe and the air temperature was measured using calibrated type K thermocouples arranged along the height of and in the centre of the cloud chamber. Several repeat pressure reduction cycles were performed once dust was inserted; after each experiment, the chamber was filled back to ambient pressure using the clean air system described above. A set of experiments for each dust was performed at both higher and lower temperature, and in total, Kaolinite,

Feldspar, and Illite were used, giving a total of 6 experiment sets comprising ~ 4 runs per set (a total of ~ 24 depressurisations, not including background runs).

3 Observations

Figures 2 and 3 show the results of the two first experimental runs on K-feldspar – the same sample used in the Atkinson et al. (2013) study. Figure 2 was conducted with the initial temperature equal to $-12\,^{\circ}\mathrm{C}$ and expansion of the air to 700 hPa resulted in the temperature decreasing to $\sim -19\,^{\circ}\mathrm{C}$. The middle plot of Fig. 2 shows the time evolution of the measured size distribution from the CDP. Mineral particles are visible at the start of the experiment at sizes up to $\sim 10\,\mu\mathrm{m}$, whereas $\sim 25\,\mathrm{s}$ into the experiment a cloud of droplets grows as noted from the brighter colours. Following the formation of drops, ice crystals are formed and grow to large sizes.

The cloud of drops evaporates at $\sim 200\,\mathrm{s}$ due to the Bergeron-Findeison process, following which the ice crystals are able to persist to $\sim 300\,\mathrm{s}$. The bottom plot of Fig. 2 shows that the drop concentration measured with the CDP reaches $\sim 2000\,\mathrm{cm}^{-3}$. The ice concentration determined by the 3V-CPI (red-line) agrees very well with the concentrations of particles greater than ~~18 µm~~ 20 µm as measured with the CDP (blue line), thus giving confidence in our measurements of ice crystal concentration. The blue-dashed line is the concentration of particles greater than 35 µm measured with the 3V-CPI. It should be noted the reason this is greater than the concentrations of particles greater than ~~18 µm~~ 20 µm measured with the CDP is because the 3V-CPI often over-sizes out of focus images of droplets (Connolly et al., 2007).

Figure 3 shows the results of the first run of K-feldspar at an initial temperature of $-21\,^{\circ}\mathrm{C}$. During the expansion the air temperature reduced to $\sim -28\,^{\circ}\mathrm{C}$. The CDP showed evidence of droplets forming for a brief period at $\sim 40\,\mathrm{s}$ in to the experiment (middle plot and black line on bottom plot). However, the droplets lasted for a brief period (less than $\sim 40\,\mathrm{s}$). The 3V-CPI concentration is lower than the CDP concentration of particles greater than ~~18 µm~~ 20 µm (blue line); however, in this experiment it was difficult to discriminate the ice crystals

on shape alone because the ice crystals appeared somewhat rounded due to the lack of vapour growth. Furthermore, the concentrations of particles greater than ~~18 µm~~20 µm, measured with the CDP, and those measured with the 3V-CPI greater than 35 µm are in good agreement. For this experiment it was more accurate to use these two measurements for the ice crystal concentrations.

Similar plots are shown in Figs. 4 and 5, but for kaolinite at $-19\,^{\circ}$C and $-25\,^{\circ}$C respectively. In Fig. 4 (middle plot) a cloud of droplets forms for ~ 50 seconds before evaporating to leave an ice cloud. It is more difficult to see from the CDP data that the ice cloud nucleates after the drops form, because the optical sizes of the ice crystals overlap with the optical sizes of the largest kaolinite particles; nevertheless the 3V-CPI data indicated that this was the case (not shown). The bottom plot of Fig. 4 shows that the 3V-CPI derived ice crystal concentration (red line) is about a factor of two smaller than the particles larger than ~~18 µm~~ 20 µm from the CDP (and those larger than 35 µm from the 3V-CPI, blue lines); this is because some of the ice crystals are too small to be able to unequivocally classify them as ice crystals on their shape alone, so we slightly underestimate the ice concentration here.

Figure 5 middle shows that the kaolinite particles nucleate ice in the absence of a cloud of droplets. In fact, the droplets are too small to see with the CDP: the humidity in the chamber was close, and likely above water saturation. The drops are not visible because the Bergeron-Findeison process acts rapidly in this experiment, leaving the drops with little time to grow. The drop mode became more visible with repeat experiments (not shown): (a) because the particle concentration was diluted and (b) because the largest, most IN active particles were used up, which enabled the drops to grow to larger sizes. As for the experiment at higher temperature the 3V-CPI derived ice crystal concentration was below that of the concentrations that were derived on size alone from the CDP and 3V-CPI (solid blue and dashed blue lines respectively). Again this is because the particle sizes were often too small to unequivocally classify them as ice; hence, we classified the ice based on size for these runs (blue lines).

Finally, we have similar plots for the NX-illite sample in Figs. 6 and 7. In Fig. 6 (top) we see that the initial temperature was $-15\,^{\circ}$C, which decreased to $\sim -23\,^{\circ}$C throughout

the experiment. The middle plot shows that the droplet mode was of fairly long duration, lasting up to $\sim 300\,s$ and that there were relatively few ice crystals (as noted from the few speckles above ~~18 µm~~ 20 µm in size). The 3V-CPI and CDP derived ice concentrations agree reasonably well in this case; however, the concentration of particles larger than 35 µm as measured with the 3V-CPI is larger than those larger than ~~18 µm~~ 20 µm measured with the CDP. The reason for this is that the 3V-CPI has a tendency to over estimate the size of the drops when they are out of focus. Drop concentrations were $\sim 2000\,cm^{-3}$.

For NX-illite at $-25\,°C$ in Fig. 7 the picture is similar to K-feldspar and kaolinite at the lower temperatures. There is no visible drop mode and the ice crystal concentration inferred from the 3V-CPI images is lower than those inferred from the CDP and 3V-CPI on size alone (bottom plot). The drop mode was visible in later expansions, when the most efficient ice nuclei had been used up and thus removed from the chamber (not shown). The reason the 3V-CPI derived ice crystal concentrations were smaller than the CDP and 3V-CPI concentrations based on size is again due to the ice crystals not developing distinct facets because there are many of them; hence, for these experiments we classified the ice on size alone (blue lines). It is noteworthy that drop concentrations were $\sim 500\,cm^{-3}$, which is lower than the aerosol by a factor of ~ 3. We suspect that NX-illite ~~had the highest~~ , because of its high specific surface area and ~~we suspect that this decreases its effectiveness~~ heteorgeneity, is less effective as a cloud condensation nucleus (CCN) ~~,~~ ~~and it perhaps even acts in the adsorption mode of CCN activation rather than in the mode described by Köhler theory (e.g. Kumar et al., 2008)~~ than the other samples, which may be explained by NX-illite having a different adsorption isotherm (e.g. Kumar et al., 2008) in comparison to the other samples.

4 Analysis

To compare our dry dispersion chamber observations with wet suspension cold stage methods (e.g. Murray et al., 2011; Broadley et al., 2012; Atkinson et al., 2013) we used two main approaches. Firstly we calculated values of the ~~ice-active-surface-site~~ ice-active surface site

density, or n_s, using our data and plotted them on the same graph as existing data taken using cold stages (see Sect. 4.1). Secondly the Aerosol-Cloud-Interactions Model (ACPIM) (Connolly et al., 2012) was used to simulate the MICC cloud chamber experiments. In this model, the freezing parameterisations of Murray et al. (2011); Broadley et al. (2012); Atkinson et al. (2013) have been implemented and were used to compare ice concentrations expected with those observed. ACPIM is discussed and the analysis is presented in Sect. 4.2.1.

4.1 Calculating n_s directly from the data

We calculated n_s directly from the data in the following way. The result of the n_s concept is that the fraction of drops, f, containing surface area, A, that are frozen at temperature, T, is described by the factor:

$$f = 1 - \exp\left(-A n_s\left[T\right]\right) \tag{1}$$

Hence, for an input dust particle size distribution, $\frac{\mathrm{d}N}{\mathrm{d}D}$, where all particles are hygroscopic, or take up at least a mono-layer of water, we write the number of ice crystals that are nucleated as:

$$N_{\text{ice}} = \int_{D_{\text{min}}}^{D_{\text{max}}} \frac{\mathrm{d}N\left(D\right)}{\mathrm{d}D}\left(1 - \exp\left(-A n_s\left[T\right]\right)\right)\mathrm{d}D \tag{2}$$

Here D_{min} and D_{max} are the minimum and maximum particle size in the mineral particle size distribution.

The value used for A in Eq. (2) is the surface area of a sphere multiplied by a factor to yield the BET specific surface area (see Table 3). We calculate n_s ~~from our data using~~ iteratively using data and Eq. (2)~~with an iterative method~~. Firstly, we use an initial guess of n_s and evaluate the integral in Eq. (2). We then compare the calculated value of N_{ice} with the measured value. This process is repeated with updates to n_s until the integral is equal to N_{ice}, at which point the method has converged.

Another way of estimating n_s (e.g. Niemand et al., 2012; Hiranuma et al., 2014) has been to divide the measured ice crystal number concentration by the surface area of the aerosol size distribution, as measured at the start of the experiment (with a pressure correction for dilution during the expansion):

$$n_s \cong \frac{N_{ice}}{\pi \int_{D_{min}}^{D_{max}} D^2 \frac{dN(D)}{dD} dD} \quad (3)$$

However, this method can lead to an underestimation of n_s because it does not take into account the removal of surface area from the dust size distribution as they nucleate ice.

The values of n_s derived using the iterative method are shown in Fig. 8. We have chosen to plot each experimental run as a single data point. Note that the spread in n_s values, for data points that are close together in temperature, arises because experiments were repeated for several expansions, which allowed the most efficient ice nuclei to be depleted from subsequent expansions. Since the ice crystal concentrations are measured with time we could use a single experiment for multiple data points as is typically done in other studies (e.g. Niemand et al., 2012; Hiranuma et al., 2014); however, we have more confidence in the accuracy of the experimentally averaged data points. It can be seen that at the higher temperatures, values from the chamber (using dry dispersion) are significantly larger than those taken from cold stages (using wet suspension). This effect has been noted for NX-illte in the recent study by Hiranuma et al. (2014).

4.2 Process modelling

The application of ACPIM to understand and interpret the implications observations is described in Sect. 4.2.1, below. The discrepancies noted in Fig. 8 prompted us to understand the reason for differences between dry-dispersion and wet-suspension techniques; hence, coagulation model calculations are presented in Sect. 4.2.2.

4.2.1 Chamber modelling

We operated ACPIM as a cloud parcel model with bin microphysics. The aerosol size distributions were specified as lognormal fits to the observed data from the UHSAS and the WELAS probes (see Table 1). The curves were ~~fitted manually~~ manually fitted to the data~~, but fitted the data very well~~. Since the background aerosol were not ice nuclei we assumed they were hygroscopic aerosol (ammonium sulphate). A single lognormal mode of ammonium sulphate aerosol was used to describe the background aerosol measured during the background experiment while ~~3~~ two lognormal modes were used to describe the mineral particle size distribution that was measured prior to the experiment. The background aerosol could be clearly distinguished from the mineral particle size distribution by size: the background distribution was narrow and had a median diameter of $\sim 40\,\mathrm{nm}$; whereas the mineral particle distribution was broad and had a median diameter of $\sim 400\,\mathrm{nm}$. It was assumed that the mineral dust had a small amount of soluble material on them, to enable them to act as cloud condensation nuclei (as well as ice nuclei). The model was relatively insensitive to the fraction of soluble material assumed in the range ~~(~~1–5 % (by mass). The parcel model was forced with the observed pressure drop rate and the temperature rate of change was calculated from the conservation of energy (1st law of thermodynamics) for moist air with the addition of a first order derivative that depends on the temperature difference between the gas and the chamber walls. In the model, total water content remained constant during an experiment (which was consistent with the condensed mass inferred from the CDP measurements and water vapour concentration measured by a tunable diode laser).

The condensation process was described by the droplet growth equation (Pruppacher and Klett, 1997), with equilibrium vapour pressures described by Köhler theory. Ice nucleation was modelled using the parameterisation of Koop et al. (2000) for homogeneous freezing or, Murray et al. (2011); Broadley et al. (2012); Atkinson et al. (2013) for heterogeneous freezing by the kaolinite, illite or feldspar mineral dust respectively. A criteria was added that a dust particle had to have 5×10^{-14} kg of water condensed before it could act in the immersion / condensation mode – this prevented ice nucleation at conditions that

were sub-saturated with respect to water, as observed. Once nucleated ice crystals grew according to the ice crystal growth equation (Pruppacher and Klett, 1997), and in this work crystals were assumed to be quasi-spherical with a variable effective density (see Connolly et al., 2012, for details). All derivatives form a large set of coupled ODEs, which were solved using the DVODE solver from Netlib.

The ACPIM model was run for every experiment in Table 1 and the results are summarised as ratios of observed to simulated ice crystal concentrations in Fig. 9. The statistics in Fig. 9 were calculated from each of the experimental runs for a particular set of experiments. In general it is shown that the parameterisations underestimate the ice crystal concentrations at all temperatures whereas from Fig. 8 one would expect the parameterisations to do reasonably well at the lower temperatures. The reason the parameterisations do not ~~to~~ do well at low temperatures is because the dry dispersion data suggest that the slope of the n_s vs temperatures curves should be shallower, thus yielding higher values of n_s at the start of the expansion.

4.2.2 Coagulation modelling

In the experimental approaches relying on wet suspension, mineral particles are added to a large volume of water and the wet suspension is stirred for ~ 12 hours with a magnetic stirrer. The drops containing mineral particles in suspension are then either sprayed (in which case pico-litre drops are produced) or pipetted onto a glass slide (in which case micro-litre drops are produced). A few minutes may then elapse before commencing the cooling of drops. Hence, it is possible that coagulation of particles happens, either in the large volume of water, or in the drops before and during the cooling cycle.

We modelled the coagulation of particles within wet-suspensions using the model described in Appendix A. We present the results here neglecting the electric double charge layer that is commonly used to describe inter-particle forces in a colloid (our justification for this is discussed in Sect. 5.1.1).

Simulations with the coagulation model were performed for 2 h run-time. We performed simulations for two weight percents (0.005 and 1.000) and also used 3 assumptions for

the size of the water drops that the mineral particles were suspended in. The first was to assume a pico-litre volume drop (1×10^{-15} m^3); the second was to assume a micro-litre volume drop (1×10^{-9} m^3) and the third was to assume an infinite volume of water. The reason for these choices was that they span the range of conditions encountered in the cold stage experiments. We also used different coagulation kernels: one where forces due to Brownian motion were the only forces governing the motion of the particles; and another where Brownian and gravitational settling forces were acting.

Figure 10 shows results from the coagulation model assuming that the forces governing the movement of mineral particles are those due to Brownian motion only. Figure 10a and b show that hardly any coagulation occurs within the pico-drops at the weight percents assumed in the calculations. This is evident from the fact that the particle sizes do not change with time. There are just too few particles present for coagulation to be efficient. When micro-litre drops are used (Fig. 10c and d) we see that the size of the mode shifts to larger sizes. This is significant for the larger weight percent drops where the median size shifts from sub-micron to 10 s of microns. The assumption of an infinite volume of water in Fig. 10e and f yields similar results to the micro-litre model run.

From the results in Fig. 10 we have calculated the ratio of mineral particle surface area to the initial mineral particle surface area. These calculations are shown in Fig. 11. We have assumed that a collision between ~~to~~ two mineral particles yields a mineral particle with the same volume as the other two and that they produce quasi-spherical particles with a fractal dimension of ~ 2 (as shown by, Vaezi G et al., 2011). Figure 11 shows that, at the highest weight percent in the micro-litre drop, the surface area of the mineral particles quickly drops to ~ 0.1 of the initial value. For the highest weight percent in the pico-litre drop and for the lowest weight percent of the micro-litre drop we see that the surface area available for nucleation is ~ 0.5 of the initial value. Finally, for the lowest weight percent in the pico-litre drop we see no reduction in the available surface area.

Figure 12 shows the same calculation of available surface area vs. time when both Brownian motion and gravitational settling influence the coagulation kernel. Similar results to those for the Brownian only kernel are shown for the pico-litre drops and also for the micro-

litre at low weight percent; however, for the micro-litre drop at high weight percent we see that the available surface area quickly drops to 0.005 of the initial value. This is in the region required to explain the discrepancies seen in Fig. 8.

It should be noted that our simulations of coagulation offer a rough calculation of the reduction in surface area due to coagulation. However, another important process to consider is the fact that, once aggregated, large particles will sediment out of the suspension; therefore further reducing the available surface area for nucleation. The subsequent calculations of n_s will be biased low because the surface area used to calculate n_s (the original surface area added to the suspension) will be too high.

4.3 Colloid experiments

In order to support our calculations we have conducted experiments where we prepare colloidal suspensions at 0.1 to 1 wt % ~~wt~~ solids (either K-feldspar, kaolinite or nx-illite) in ultrapure (18.2 MΩ cm) water.

We stirred the suspensions for 12 h using a magnetic stirrer to reproduce the methods of previous ice nucleation studies and then passed them through either 1 µm or 5 µm filters (22 mm Cellulose nitrate membrane, Whatman, UK). We found in all cases that this process reduced the absorbance of UV and visible light to that of ultrapure water (UV-Vis spectrometer, Stellarnet, Fla., USA) and, therefore, removed the particles completely to within error of the absorbance measurements. Less than 2 ml of suspension was passed through the filter membranes and their effective pore-size would have remained unaltered. This, therefore, suggests that the particles had aggregated from their initial sub-micron sizes to super micron sizes. We also monitored the absorbance of the suspension vs time across the spectrum; at 567 nm, the optimum wavelength with respect to signal to noise, and found it to decrease by a factor of 10 within 90 min of sample preparation. This also suggests that sedimentation and aggregation had occurred.

Measurements were performed using a Malvern Zetasizer Nano ZS at the University of Manchester, UK. Kaolinite suspensions were prepared (MilliQ H2O and 100 mM NaCl) to study the effect of electrolytes on particle aggregation. The water was filtered with a 0.2 µm

PTFE filter to eliminate possible dust particles. Measurements of the kaolinite samples were conducted with concentrations of 0.1, 0.33 and 1 mg ml^{-1} (0.01, 0.033 and 0.1 wt %~~by wt~~) prepared by mild sonication for 5 min at 60 °C then immediately cooled to room temperature and measured within minutes. Note that in the absence of heating to 60 °C the particles remained in an aggregated state. The pH was varied between 3 and 11 by addition of the minimum amount of diluted HCl or NaOH, respectively and the results are summarised in Table 2.

Measurements in MilliQ water show an increase in particle size with increasing kaolinite concentration. It is notable that at pH $\sim$ 9.0 there is a factor of two increase in particle size going from 0.33 mg ml^{-1} concentration to 1 mg ml^{-1} since the pH of kaolinite in MilliQ water was measured to be $\sim$ 8.2 in the aggregated sample; thus suggesting that aggregation is important. The effect of electrolytes is clearly seen in the lower half of Table 2. At high NaCl concentrations aggregation is enhanced, as expected, since charges on the clay minerals are neutralized by the mobile charges in solution. It is not clear whether this enhancement in aggregation is due to a reduction in like-like charge repulsion or an enhancement in the attraction of particles with different zeta-potential in the heterogeneous mineral particle sample (see Appendix C, Fig. 13).

5 Discussion

Recently Hiranuma et al. (2014) suggested that there is a discrepancy between the dry-dispersion and wet-suspension methods of determining the ice nucleation efficiency of the clay mineral NX-illite. They ~~offered the explanation~~ explained that the mineral surface is chemically altered during reaction with water, which may affect the ice nucleating activity. Their measurements of ion concentrations in water containing NX-illite supported this finding; however, ~~their water was acidic to speed up the breakdown of the mineral surface. Here we find the same result for the same NX-illite sample. We also find very similar results for K-feldspar and kaolinite KGa-1b samples. Namely~~ since ion concentrations are able to screen surface charge on colloidal particles these charges may significantly enhance

the ability of the particles to coagulate (see Appendix B and C). We also confirm that the dry-dispersion method we used predicts higher values of n_s than the previously published results using wet-suspensions at ~~the highest~~ high temperatures, but ~~agrees~~ that the two methods are in close agreement at the lower temperatures. We offer an alternate explanation to that of Hiranuma et al. (2014), which is that the mineral particles may coagulate together in suspension and reduce the surface area available for nucleation.

This explanation is also consistent with the discrepancy found at high temperatures: in the wet-suspension methods, the high temperature results use the highest mineral particle weight percents, which are more likely to coagulate. However, Atkinson et al. (2013) show that high weight percents (0.8 %) in pico-litre drops at lower temperatures that agree with our dry-dispersion measurements. We suggest ~~that the~~ a possible reason is that the ~~mineral particles are prevented from coagulation by the stirring process but that they coagulate in a period of a few minutes after being pippeted onto the glass side~~K-feldspar particles form relatively weak aggregates, which can be disrupted and broken up by energetic spraying into pico-litre size drops, but not by pipetting into micro-litre drops. This may explain (with reference to Fig. 12) why the pico-litre drops at high weight percent presented in Atkinson et al. (2013) agrees with our measurements, but the micro-litre drops at the same weight percent do not. Coagulation can also occur within micro-litre drops, but tends not to in pico litre drops because they lack sufficient mineral particles for the process to be efficient. Another alternate explanation is that the spraying process for the pico-litre drops causes the aggregates to be disrupted.

5.1 Does the assumption of spherical particles affect our findings?

We note that Fig. 8 is adjusted so that we take account of the specific surface area; however, the process modelling (Fig. 9) assumes the surface area of spherical mineral particles. Here we assess whether this affects the main findings. The quoted values for BET specific surface areas of the three samples are shown in Table 3.

We estimate the discrepancy in the assumption that the particles are spherical. The median diameter for the three samples when introduced into the chamber was approximately

$D_{\mathrm{m}} = 0.4 \times 10^{-6}$ m. The calculated surface area to mass ratio is then, S:

$$S = \frac{6\cancel{D_{\mathrm{m}}^2}}{\rho\cancel{D_{\mathrm{m}}^3}} \tag{4}$$

$$= \frac{6}{\rho D_{\mathrm{m}}} \tag{5}$$

We may then calculate the SSA underestimation factor, which is the ratio of the SSA to the value of S. Table 3 shows that the assumption of spherical particles likely underestimates the surface area for the kaolinite and NX-illite samples by factors of ~ 2 and ~ 20 respectively. For the K-feldspar the assumption of sphericity overestimates the surface area by a factor of ~ 2. The underestimation is because the particles are platelets so measured optical size is closer to $\frac{\pi D^2}{2}$ (area of a disk) instead of πD^2 (area of a sphere). It should be noted that these values are not large enough to significantly affect the conclusions from Fig. 9.

5.1.1 Colloidal forces in suspensions

The coagulation modelling in Sect. 4.2.2 neglected the force of repulsion due to the electric double charge layer (see Appendix B and C for details). Kaolinite is a 1:1 layer clay consisting of alternating silca (tetrahedral) and alumina (octahedral) layers, which are bonded together. The tetrahedral faces have a net negative charge due to isomorphic substitution of silicon ions by ions with a lower charge, whereas the edges and octahedral faces have charges that depend on the pH of the solution.

When placed in suspension the minerals develop a double charge layer by attracting positive ions (counter-ions) to the surface. The double charge layer can result in the particles being colloidally stable because of the effective like-charge Coulomb interaction between two particles. The sign and magnitude of the charge layer can be quantified by inferring the zeta-potential from measurements of electro-phoresis.

We now provide some justification for the decision to neglect it. Elimelech et al. (2000) have shown that the ζ-potential is a relatively insignificant factor in predicting the transport

/ sedimentation of particles when there is heterogeneity in the surface of the colloidal material. This is reasonable since the ζ-potential is only a bulk measurement of the charge on a population of particles.

Tombácz and Szekeres (2006) have since shown that kaolinite has surface charge heterogeneity due to the mineral having permanent charges on the tetrahedral silica faces and pH dependent charges on the crystal edges and also the octahedral alumina faces. In the paper by Tombácz and Szekeres (2006), kaolinite samples were heavily processed to remove the large particle sizes and any other contamination; however, surface charge heterogeneity still persisted.

The faces of alumina and edges of the kaolinite crystal may undergo hydrolysis and hence carry pH dependent charges (Tombácz and Szekeres, 2006). Tombácz and Szekeres (2006, their Fig. 7) show that, at pH 7, these alumina and silica groups (as inferred through a linear combination of their zeta potential) may have an overall charge close to zero. Hence, there is surface charge heterogeneity in clay minerals. Indeed Schofield and Samson (1954) had noted previously that "edge to face" coagulation (or flocculation) occurs in kaolinite samples.

Berka and Rice (2005) have shown that kaolinite can be colloidally stabilized at particle concentrations similar to those under consideration here ($\sim 10^{16}\,\mathrm{m}^{-3}$); however, their results are at pH of 9.5, where the alumina also carries high negative charge; hence, it should be expected that kaolinite will be colloidally stabilized to some extent at pH 9.5. Our own dynamic light scattering measurements confirm that high pH does cause some colloidal stability, but that this can be overcome at higher concentrations (Table 2).

6 Conclusions

Experiments were conducted in the Manchester Ice Cloud Chamber facility to look at ice nucleation in the condensation mode. Three dusts were investigated: kaolinite, illite, and feldspar, and each dust was examined at relatively high and low temperatures. The primary

goal of this study was to reconcile dry-dispersion methods of quantifying ice nucleation on mineral dusts with those using wet-suspension.

Observations revealed feldspar to be the most efficient dust at nucleating ice (Fig. 8) in agreement with Atkinson et al. (2013), followed by illite, then kaolinite. Thus our data are qualitatively in agreement with previous findings. However, they all showed a discrepancy at the higher temperatures; the dry dispersion methods always showed higher values of n_s than the wet-suspension methods.

Using the ACPIM numerical model to simulate the cloud chamber with ice nucleation parameterisations provided by Murray et al. (2011); Broadley et al. (2012), ice concentrations for all dusts were underestimated relative to observations. The reason for this was that the slope of the n_s vs. temperature curves were determined to be less steep in our measurements than the wet-suspension methods. Hence, the reason the model under-predicted the ice crystal concentration at lower temperatures was because the values of n_s from the parameterisations were too low at the start of the experiment. Thus too few ice crystals were nucleated and by the time the lower temperatures were reached the Bergeron–Findeison process had led to the evaporation of the drops.

Modelling of coagulation in suspension showed that it may be a pathway to significantly reduce the surface area of mineral particles and hence would reduce the effective n_s calculated from experimental data. This is confirmed by separate experiments passing the suspensions through filters after initial dispersion and also through dynamic light scattering.

To explain the discrepancy between dry-dispersions and wet-suspensions we suggest the following:

- During the stirring process feldspar particles do not ~~coagulate strongly and remain in suspension~~ adhere strongly to each other. These weak aggregates may thus be easily disrupted when pico litre drops of the suspension are sprayed, because the drops are a similar size to the aggregate particles in this case.

- Illite and kaolinite particles ~~may behave differently and could coagulate~~ form stronger, more tightly packed, aggregates and could sediment during the stirring process.
- At high concentrations $\sim 1.000\,\mathrm{wt}\,\%$ coagulation is more likely to happen.
- As the drops are either sprayed, or ~~pippetted~~ pipetted onto the glass slide the mineral particles within the drops may start to coagulate. ~~Another alternate explanation is that aggregation does happen during stirring, but that energetic spraying of the pico litre sized drops results in the aggregate particles breaking up.~~
- After generation of the pico-litre drops they contain insufficient mineral particles, even at $1.000\,\mathrm{wt}\,\%$, to result in significant coagulation.
- In micro-litre drops there are enough mineral particles to result in significant coagulation, and a reduction of surface area in the drops. This reduction increases with increasing wt % of mineral particles.
- The slopes of the n_s vs temperature derived from our dry dispersion experiments more closely agree with those derived for natural dusts by Niemand et al. (2012).
- The dry-dispersion techniques suggest that mineral particles are more efficient than the wet-suspension derived parameterisations suggest, especially at relatively high temperatures.

Appendix A: Modelling coagulation in suspension

We adopted the semi-implicit numerical algorithm for treating the coagulation process (pp 438 Jacobson, 1999). This method conserves total particle volume and approximately conserves the monomer concentration. The algorithm is written as follows:

$$v_{k,t} = \frac{v_{k,t-1} + \mathrm{d}t \sum_{j=1}^{k} \left(\sum_{i=1}^{k-1} f_{i,j,k} \beta_{i,j} v_{i,t} n_{j,t-1} \right)}{1 + \mathrm{d}t \sum_{j=1}^{N_\mathrm{B}} \left(1 - f_{k,j,k}\right) \beta_{k,j} n_{j,t-1}} \tag{A1}$$

with $n_k = \frac{v_k}{\nu_k}$ and:

$$f_{i,j,k} = \begin{cases} \left(\frac{\nu_{k+1}-V_{i,j}}{\nu_{k+1}-\nu_k}\right)\frac{\nu_k}{V_{i,j}} & \nu_k \le V_{i,j} < \nu_{k+1} \text{ if } k < N_\mathsf{B} \\ 1 - f_{i,j,k-1} & \nu_{k-1} < V_{i,j} < \nu_k \text{ if } k > 1 \\ 1 & V_{i,j} \ge \nu_k \text{ if } k = N_\mathsf{B} \\ 0 & \text{all other cases} \end{cases} \tag{A2}$$

Equation (A1) shows that the solution at the next time-step depends on the solution at that time-step; hence, the method is an "implicit" method; however, the algorithm is solve sequentially in discrete bins such that the solution at the next time-step is always known.

The variable β is the coagulation kernel of two interacting particles ($\mathrm{m}^3\,\mathrm{particle}^{-1}\,\mathrm{s}^{-1}$). When by the concentration of particles in a discrete bin it gives the rate of the number of particle interactions. We assume it can be described by the sum of a kernel due to Brownian diffusion and that due to gravitational settling. For Brownian the diffusion the kernel takes the form:

$$\beta(i,j) = 4\pi\left(r_i + r_j\right)\left(D_{\mathsf{p},i} + D_{\mathsf{p},j}\right) \tag{A3}$$

where $D_{\mathsf{p},i}$ and $D_{\mathsf{p},j}$ are particle diffusion coefficients:

$$D_{\mathsf{p},i} = \frac{k_\mathsf{B} T}{6\pi r_i \eta_\mathsf{w}} \tag{A4}$$

following Einstein (1956). This model assumes that each Brownian collision results in a sticking event.

For gravitational settling the kernel takes the form:

$$\beta(i,j) = E_{i,j}\pi\left(r_i + r_j\right)^2 \left|u_{t,i} - u_{t,j}\right| \tag{A5}$$

Appendix B: Interaction potential of minerals in suspension

A particle suspended in water will generally form a double charge layer by accumulation of ions.

The potential energy of the electrical double layer interaction between two spheres may be written:

$$V_R = \left(\frac{\pi\epsilon R_1 R_2}{R_1 + R_2}\right)\left(\zeta_1^2 + \zeta_2^2\right)\left(\frac{2\zeta_1\zeta_2}{\zeta_1^2 + \zeta_2^2}p + q\right) \tag{B1}$$

where R_1 and R_2 are the radii of the two interacting particles; ϵ is the electric permittivity; $\zeta_{1,2}$ are the zeta potentials of the interacting particles.

$$p = \ln\left(\frac{1 + \exp(-\kappa x)}{1 - \exp(-\kappa x)}\right) \tag{B2}$$

$$q = \ln\left(1 - \exp(-2\kappa x)\right) \tag{B3}$$

where x is the shortest distance between to particles and κ^{-1} is the Debye length:

$$\kappa^{-1} = \sqrt{\frac{\epsilon k_B T}{N_A e^2 \sum Z^2 m_i}} \tag{B4}$$

where k_B is Boltzmann's constant; N_A is Avogadros' number, $e = 1.6\times10^{-19}$ C is the charge on an electron; Z and m_i are the valence and molar concentration (moles per cubic metre) of ions; and T is the temperature.

In addition to the electrical double layer potential we also consider the van der Waals interaction, which is given by London's equation:

$$V_A = -\frac{A_{132}}{6}\left(\frac{2R_1R_2}{[R_1+R_2+x]^2+[R_1+R_2]^2} + \frac{2R_1R_2}{[R_1+R_2+x]^2+[R_1-R_2]^2} + \ln\left[\frac{[R_1+R_2+x]^2+[R_1+R_2]^2}{[R_1+R_2+x]^2+[R_1-R_2]^2}\right]\right) \tag{B5}$$

here, A_{132} is the Hamaker constant for interaction between particle 1, particle 2 in medium 3. Individual Hamaker constants are as follows: for mineral particles we use A_1 and $A_2 = 6.8 \times 10^{-19}$ J; whereas for pure water we use $A_3 = 7 \times 10^{-21}$ J. A_{132} can be estimated (source) from the Hamaker constants for pure components:

$$A_{132} \cong \left(\sqrt{A_1} - \sqrt{A_3}\right)\left(\sqrt{A_2} - \sqrt{A_3}\right) \tag{B6}$$

The total potential for the interaction is given by the sum of van der Waals and the double electric charge layer: $V_\mathrm{T} = V_A + V_R$.

Appendix C: Coagulation kernel with interaction potential

As described in Housiadas and Drossinos (2005, Sect. 6.3.1.2) the coagulation kernel can be corrected for the effect of an external, conservative force field. Here, "external" refers to the force field being external to the process considered in the uncorrected kernel. The correction is to divide the kernel by the factor:

$$Q = (R_i + R_j)\int_0^\infty \frac{\exp\left[\frac{V_\mathrm{T}(x)}{k_\mathrm{B}T}\right]}{x^2}\mathrm{d_x} \tag{C1}$$

We define the enhancement factor over the Brownian kernel, W, as the ratio of Q calculated with the interaction potential in Eqs. (B1) and (B5) to that calculated by van der Waals alone (B5). This enhancement factor is shown in Fig. 13 for two, spherical, $0.1\,\mu m$ diameter, particles having different values of the zeta-potential.

Figure 13 shows that two particles may come together if the zeta-potential of one of the particles has a magnitude less than a threshold of $\sim 10\,mV$. However, mineral particles are not spheres and exhibit patch-wise heterogeneity in their surface potential (see Sect. 5.1.1). Hence, we argue that for measured bulk zeta-potentials of $-20\,mV$ there may be enough heterogeneity in the sample, in addition to patch-wise heterogeneity, to lead to colloidal instability.

In addition Fig. 13 also shows that the enhancement factor may be greater than unity even when the particles have like change. This is seen most clearly at values of $\zeta_1 \cong -20\,mV$ and $\zeta_2 \cong 0\,mV$, where the enhancement factor is ~ 5. This behaviour is because the interaction between the two spheres produces induced charges, and has been observed experimentally in other studies.

Acknowledgements. This work was funded by the NERC ACID-PRUF programme, grant code NE/I020121/1. We also acknowledge funding from the EU FP7-ENV-2013 programme "impact of Biogenic vs. Anthropogenic emissions on Clouds and Climate: towards a Holistic UnderStanding" (BACCHUS), project (number 603445). Ben Murray is acknowledged for providing the mineral particle samples sourced from the clay mineral society~~and for commenting on an early draft of this work~~.

References

Atkinson, J. D., Murray, B. J., Woodhouse, M. T., Whale, T. F., Baustian, K. J., Carslaw, K. S., Dobbie, S., O'Sullivan, D., and Malkin, T. L.: The importance of feldspar for ice nucleation by mineral dust in mixed-phase clouds, Nature, 498, 355–358, 2013.

Berka, M. and Rice, J. a.: Relation between aggregation kinetics and the structure of kaolinite aggregates., Langmuir, 21, 1223–1229, doi:10.1021/la0478853, 2005.

Broadley, S. L., Murray, B. J., Herbert, R. J., Atkinson, J. D., Dobbie, S., Malkin, T. L., Condliffe, E., and Neve, L.: Immersion mode heterogeneous ice nucleation by an illite rich powder representative of atmospheric mineral dust, Atmos. Chem. Phys., 12, 287–307, doi:10.5194/acp-12-287-2012, 2012.

Connolly, P. J., Flynn, M. J., Ulanowski, Z., Choularton, T. W., Gallagher, M. W., and Bower, K. N.: Calibration of the Cloud Particle Imager Probes using calibration beads and Ice Crystal Analogs: The depth-of-field, J. Atmos. Ocean. Tech., 24, 1860–1879, 2007.

Connolly, P. J., Möhler, O., Field, P. R., Saathoff, H., Burgess, R., Choularton, T., and Gallagher, M.: Studies of heterogeneous freezing by three different desert dust samples, Atmos. Chem. Phys., 9, 2805–2824, doi:10.5194/acp-9-2805-2009, 2009.

Connolly, P. J., Emersic, C., and Field, P. R.: A laboratory investigation into the aggregation efficiency of small ice crystals, Atmos. Chem. Phys., 12, 2055–2076, doi:10.5194/acp-12-2055-2012, 2012.

Einstein, A.: Investigations on the Theory of the Brownian Movement, Dover publications, New York, United States, 1956.

Elimelech, M., Nagai, M., Ko, C.-H., and Ryan, J. N.: Relative insignificance of mineral grain zeta potential to colloid transport in geochemically heterogeneous porous media, Environ. Sci. Technol., 34, 2143–2148, 2000.

Glaccum, R. A. and Prospero, J. M.: Saharan aerosol over the tropical north atlantic – mineralogy, Mar. Geol., 37, 295–321, 1980.

Hiranuma, N., Augustin-Bauditz, S., Bingemer, H., Budke, C., Curtius, J., Danielczok, A., Diehl, K., Dreischmeier, K., Ebert, M., Frank, F., Hoffmann, N., Kandler, K., Kiselev, A., Koop, T., Leisner, T., Möhler, O., Nillius, B., Peckhaus, A., Rose, D., Weinbruch, S., Wex, H., Boose, Y., DeMott, P. J., Hader, J. D., Hill, T. C. J., Kanji, Z. A., Kulkarni, G., Levin, E. J. T., McCluskey, C. S., Murakami, M., Murray, B. J., Niedermeier, D., Petters, M. D., O'Sullivan, D., Saito, A., Schill, G. P., Tajiri, T., Tolbert, M. A., Welti, A., Whale, T. F., Wright, T. P., and Yamashita, K.: A comprehensive laboratory study on the immersion freezing behavior of illite NX particles: a comparison of seventeen ice nucleation measurement techniques, Atmos. Chem. Phys. Discuss., 14, 22045–22116, doi:10.5194/acpd-14-22045-2014, 2014.

Housiadas, C. and Drossinos, Y.: Multiphase Flow Handbook, edited by: Clayton T. Crowe, CRC-Press, 6-1 -6-58, ISBN 9780849312809, http://www.crcnetbase.com/isbn/9781420040470, Sep 2005.

Jacobson, M. Z.: Fundamentals of Atmospheric Modelling, Cambridge University Press, Cambridge, UK, 1999.

Kandler, K., Benker, N., Bundke, U., Cuevas, E., Ebert, M., Knippertz, P., Rodriguez, S., Schutz, L., and Weinbruch, S.: Chemical composition and complex refractive index of Saharan mineral dust at Izana, Tenerife (Spain) derived by electron microscopy, Atmos. Environ., 41, 8058–8074, doi:10.1016/j.atmosenv.2007.06.047, 2007.

Koop, T., Luo, B., Tsias, A., and Peter, T.: Water activity as the determinant for homogeneous ice nucleation in aqueous solutions, Nature, 406, 611–614, 2000.

Kumar, P., Sokolik, I. N., and Nenes, A.: Parameterization of cloud droplet formation for global and regional models: including adsorption activation from insoluble CCN, Atmos. Chem. Phys., 9, 2517–2532, doi:10.5194/acp-9-2517-2009, 2009.

Murray, B. J., Broadley, S. L., Wilson, T. W., Atkinson, J. D., and Wills, R. H.: Heterogeneous freezing of water droplets containing kaolinite particles, Atmos. Chem. Phys., 11, 4191–4207, doi:10.5194/acp-11-4191-2011, 2011.

Niemand, M., Möhler, O., Vogel, B., Vogel, H., Hoose, C., Connolly, P. J., Klein, H., Bingemer, H., DeMott, P. J., Skotzki, J., and Leisner, T.: A particle-surface-area-based parameterisation of immersion freezing on mineral dust particles, J. Atmos. Sci., 69, 2012.

Pruppacher, H. R. and Klett, J. D.: Microphysics of Clouds and Precipitation, Kluwer Academic Press, Norwell, 1997.

Schofield, R. K. and Samson, H. R.: Flocculation of kaolinite due to the attraction of oppositely charged crystal faces, Discuss. Faraday Soc., 18, 135–145, doi:10.1039/DF9541800135, 1954.

Tombácz, E. and Szekeres, M.: Surface charge heterogeneity of kaolinite in aqueous suspension in comparison with montmorillonite, Appl. Clay Sci., 34, 105–124, doi:10.1016/j.clay.2006.05.009, 2006.

Vaezi G, F., Sanders, R. S., and Masliyah, J. H.: Flocculation kinetics and aggregate structure of kaolinite mixtures in laminar tube flow, J. Colloid Interf. Sci., 355, 96–105, doi:10.1016/j.jcis.2010.11.068, 2011.

Vali, G.: Supercooling of water and nucleation of ice (drop freezer), Am. J. Phys., 39, 1125–1128, 1971.

Table 1. Table showing summary of experimental results. Ice crystal concentrations are determined from the CPI number concentration of ice crystals, unless stated otherwise. Multiple rows indicate the expansion number on the same mineral particle sample after refilling to 1000 hPa. Geometric surface areas were obtained through integration of the size distribution assuming spherical particles. Errors in ice crystal concentration are calculating using Poisson counting statistics at the 0.05 level of significance.

Mineral sample	ice conc. (cm^{-3})	N (cm^{-3})	D_m (μm)	$\ln \sigma_g$	Geometric surface area (m^{-1})
K-feldspar @ $-12\,^{\circ}C$	8.96 ± 0.15	[1700, 45]	[0.32, 2.8]	[0.3, 0.55]	1.99×10^{-3}
	6.31 ± 0.13	[1200, 15]	[0.32, 2.8]	[0.5, 0.55]	1.25×10^{-3}
	4.53 ± 0.11	[800, 4]	[0.32, 2.8]	[0.5, 0.45]	5.75×10^{-4}
	2.56 ± 0.08	[400, 3]	[0.32, 2.8]	[0.5, 0.65]	3.44×10^{-4}
K-feldspar @ $-21\,^{\circ}C$ [a]	47.16 ± 0.35	[1000, 20]	[0.32, 2.8]	[0.5, 0.8]	1.41×10^{-3}
	53.39 ± 0.38	[600, 20]	[0.33, 1.0]	[0.45, 1.5]	7.03×10^{-4}
	32.56 ± 0.29	[300, 20]	[0.33, 1.0]	[0.45, 1.4]	5.42×10^{-4}
	27.05 ± 0.27	[200, 1]	[0.33, 1.0]	[0.45, 0.8]	1.10×10^{-4}
Kaolinite@ $-19\,^{\circ}C$	9.51 ± 0.16	[500, 90]	[0.45, 2.8]	[0.4, 0.6]	4.35×10^{-3}
	1.52 ± 0.06	[300, 20]	[0.45, 2.8]	[0.4, 0.5]	1.13×10^{-3}
	0.34 ± 0.03	[200, 8]	[0.45, 2.8]	[0.4, 0.5]	5.50×10^{-4}
	0.20 ± 0.02	[100, 15]	[0.45, 2.8]	[0.4, 0.55]	7.23×10^{-4}
	0.06 ± 0.01	[50, 5]	[0.45, 2.8]	[0.4, 0.8]	2.81×10^{-4}
Kaolinite@ $-25\,^{\circ}C$	5.29 ± 0.12	[500, 90]	[0.4, 3]	[0.4, 0.6]	4.55×10^{-3}
	8.43 ± 0.15	[375, 60]	[0.45, 3]	[0.4, 0.6]	3.21×10^{-3}
	8.59 ± 0.15	[250, 40]	[0.5, 2.8]	[0.4, 0.65]	2.11×10^{-3}
	8.78 ± 0.15	[150, 25]	[0.45, 2.8]	[0.4, 0.8]	1.28×10^{-3}
	4.69 ± 0.11	[50, 15]	[0.45, 2.8]	[0.5, 0.8]	7.26×10^{-4}
Illite@ $-15\,^{\circ}C$	1.59 ± 0.07	[1400, 15]	[0.28, 2.6]	[0.25, 0.5]	5.10×10^{-4}
	0.182 ± 0.02	[700, 5]	[0.27, 2.6]	[0.28, 1.3]	1.92×10^{-4}
	0.037 ± 0.01	[400, 2]	[0.27, 2.6]	[0.48, 0.5]	1.73×10^{-4}
	0.021 ± 0.03	[250, 3]	[0.27, 2.6]	[0.48, 2]	1.50×10^{-4}
Illite@ $-25\,^{\circ}C$	8.04 ± 0.15	[1700, 25]	[0.28, 3]	[0.45, 0.5]	1.51×10^{-3}
	10.36 ± 0.17	[1500, 20]	[0.28, 3]	[0.45, 1]	1.27×10^{-3}
	10.92 ± 0.17	[800, 15]	[0.28, 3]	[0.45, 1.6]	7.14×10^{-4}

[a] Ice concentrations determined from particles greater than 20 μm as measured with the CDP for this experiment because the concentrations were high and hence the ice crystal sizes were small.

Table 2. Table showing results from dynamic light scattering experiments for the kaolinite sample.

In water			
pH	diameter for 0.1 mg ml^{-1} (nm)	diameter for 0.33 mg ml^{-1} (nm)	diameter for 1 mg ml^{-1} (nm)
3.0	692.4	1143.0	1777.0
5.1	652.1	741.9	753.2
7.0	695.0	742.4	792.8
9.0	449.4	418.0	721.6
11.0	467.7	448.0	693.2
100 mM NaCl			
pH	diameter for 0.1 mg ml^{-1} (nm)	diameter for 0.33 mg ml^{-1} (nm)	
3.0	1241.5	1585.0	
5.1	913.0	1318.5	
7.0	740.1	1533.5	
9.1	674.6	1350.0	
11.0	618.2	997.85	

Table 3. Table showing BET specific surface area of the different mineral samples used in this study.

Mineral sample	BET SSA $m^2\ kg^{-1}$	Bulk density ($kg\ m^{-3}$)	SSA underestimation factor
Kaolinite	11 800	2650	~ 2.1
NX-Illite	104 200	2770	~ 19.2
K-feldspar	3115 [a]	2570	~ 0.53

[a] 3.5 times that of 890.

Table 4. Nomenclature.

β	Coagulation kernel (m^3 particle^{-1} s^{-1})	Eq. (A1)
ϵ	Permittivity of water (F m^{-1})	Eq. (B4)
η_w	Viscosity of water $\sim 8.9 \times 10^{-4}$ Pa s	Eq. (A4)
κ	Reciprocal of Debye length (m^{-1})	Eq. (B2)
ν	The volume of a single particle in a bin (m^3)	Eq. (A1)
ζ_1	zeta potential of particle 1 (V)	Eq. (B1)
ζ_2	zeta potential of particle 2 (V)	Eq. (B1)
A_1, A_2	Hamaker constant for particles 1 and 2 (6.8×10^{-19} J)	Eq. (B5)
A_3	Hamaker constant for water (7×10^{-21} J)	Eq. (B5)
A_{132}	Hamaker constant for interaction between particle 1 and 2 in medium 3	Eq. (B5)
$D_{p,i}$	Particle diffusion coefficient (Stokes–Einstein coefficient) for bin i (m^2 s^{-1})	Eq. (A3)
e	Charge on electron ($\sim 1.6 \times 10^{-19}$ C)	Eq. (B4)
k_B	Boltzmann's constant, 1.381×10^{-23} m^2 kg s^{-2} K^{-1}	Eq. (A3)
m_i	Molar concentration of ions (mol m^{-3})	Eq. (B4)
N_A	Avogadros number (6.02×10^{23})	Eq. (B4)
N_B	The number of bins	Eq. (A2)
R_1	Radius of particle 1 (m)	Eq. (B1)
R_2	Radius of particle 2 (m)	Eq. (B1)
$r_{i,j}$	The radius of a particle in bin i or j (m)	Eq. (A3)
T	Temperature (K)	Eq. (B4)
u	Terminal velocity of particle in fluid (m s^{-1})	Eq. (A5)
V	The volume of the bin edges (m^3)	Eq. (A2)
n	The number concentration of a particle in a bin (m^{-3})	Eq. (A1)
v	The total volume all particles in a bin (m^3 m^{-3})	Eq. (A1)
V_A	van der Waals interaction potential (V)	Eq. (B5)
V_R	Interaction potential between two particles (V)	Eq. (B1)
V_T	Sum of all interaction potentials (V)	Eq. (C1)
W	Correction factor for particles interacting with potential	Eq. (C1)
Z	Valence of dissociation	Eq. (B4)
x	Distance between two particles (m)	Eq. (B2)

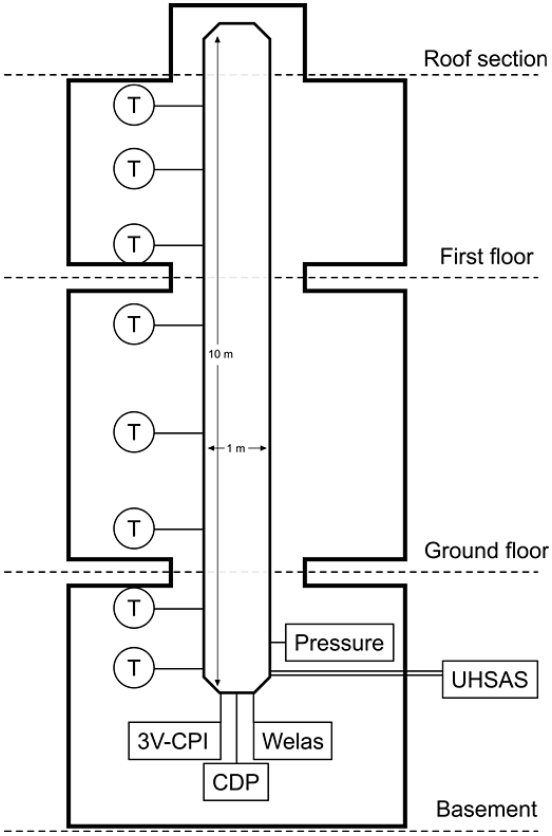

Figure 1. A schematic of the MICC cold-rooms and chamber. Outer lines mark the outline of the outer wall of the cold rooms, with the MICC tube inside. Temperature probes are labeled with a "T". Pressure, and cloud properties are monitor in the bottom section of the chamber.

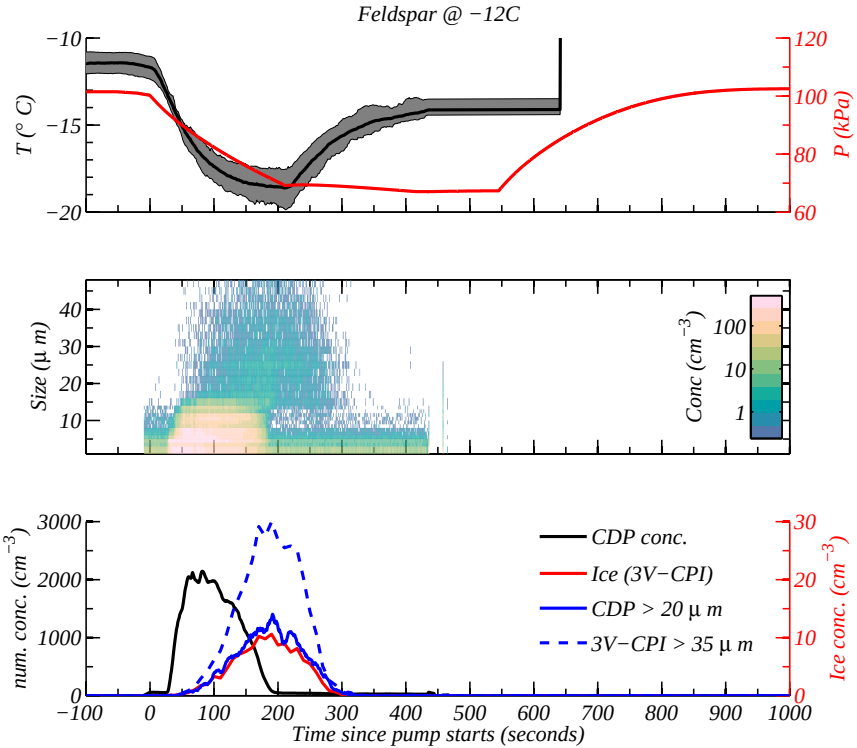

Figure 2. Feldspar mineral particles at −12 °C. Top shows the temperature in the chamber (black line, left axis) and the pressure (red line, right axis). The black line is the mean of temperature probes, while the grey shading demarks the range in measured temperatures across all probes. Middle plot shows the size distribution as measured with the CDP instrument. Bottom plot shows: (1) the drop concentration measured with the CDP (black line, left axis); (2) the concentration of particles larger than the main droplet mode (solid blue line, right axis); (3) the ice crystal concentration measured with the 3V-CPI (red line, right axis); (4) the concentration of particles larger than 35 microns with the 3V-CPI (dotted blue, right axis).

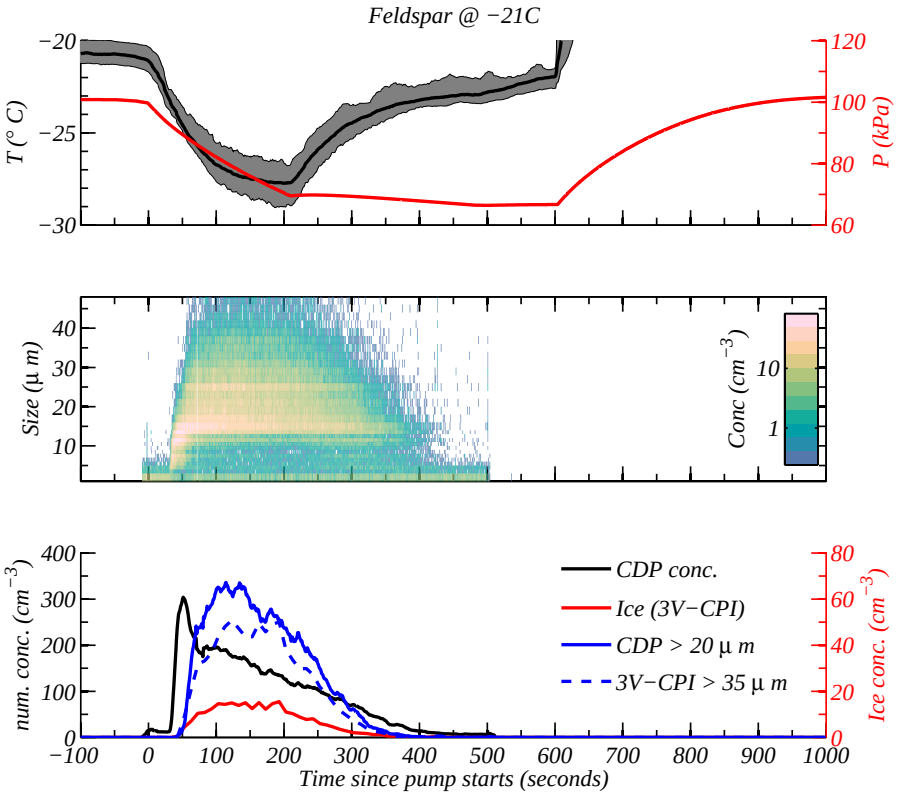

Figure 3. Same as Fig. 2, but for feldspar at −21 °C.

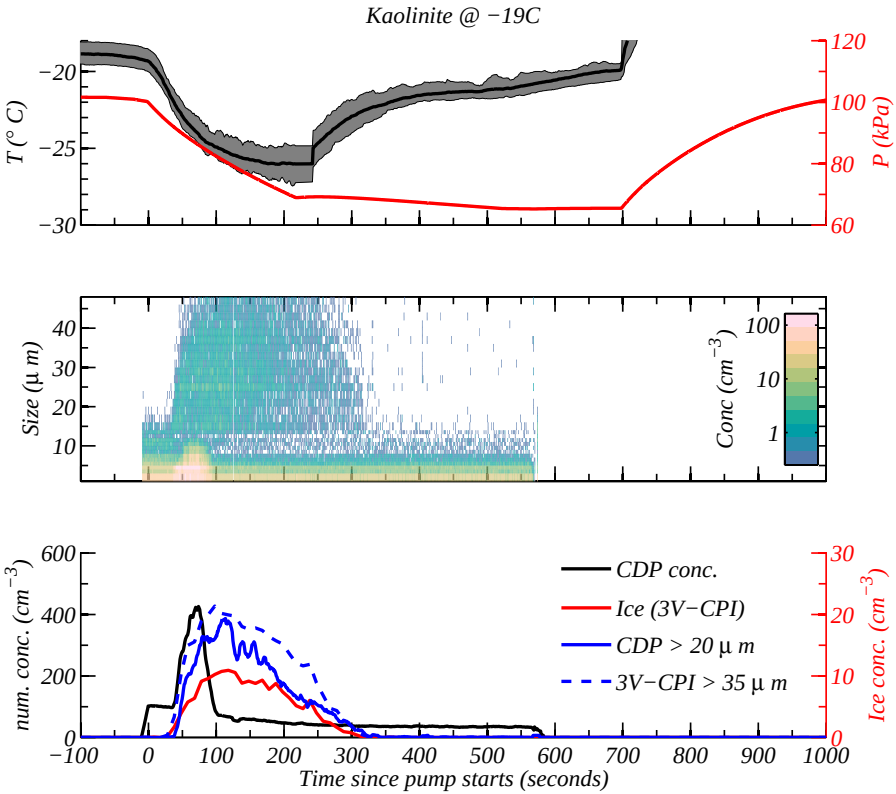

Figure 4. Same as Fig. 2, but for kaolinite at −19 °C.

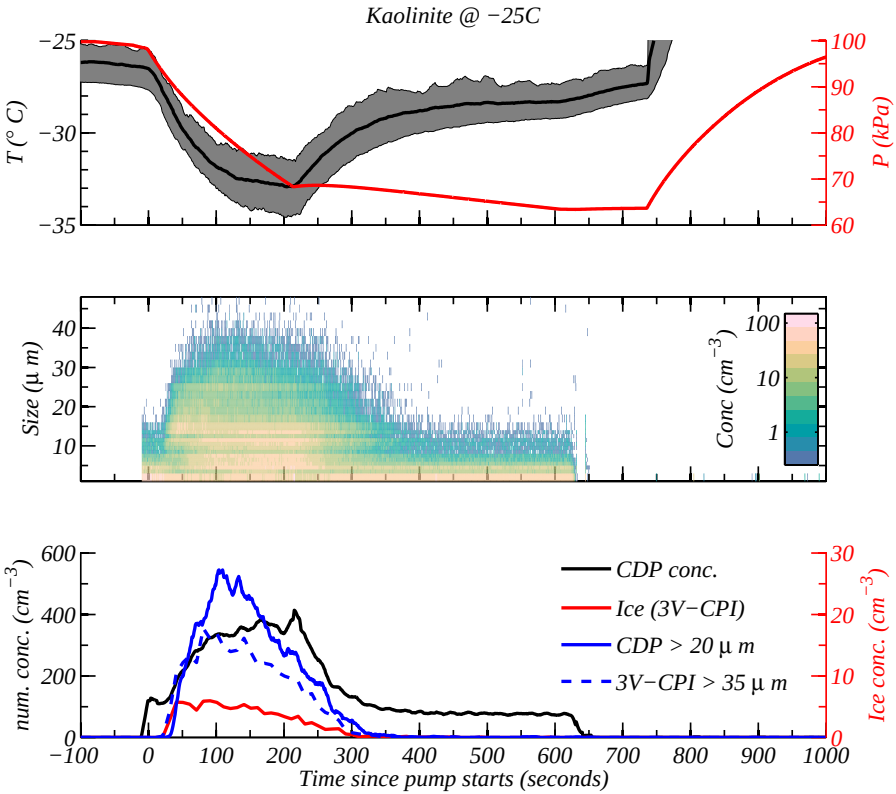

Figure 5. Same as Fig. 2, but for kaolinite at −25 °C.

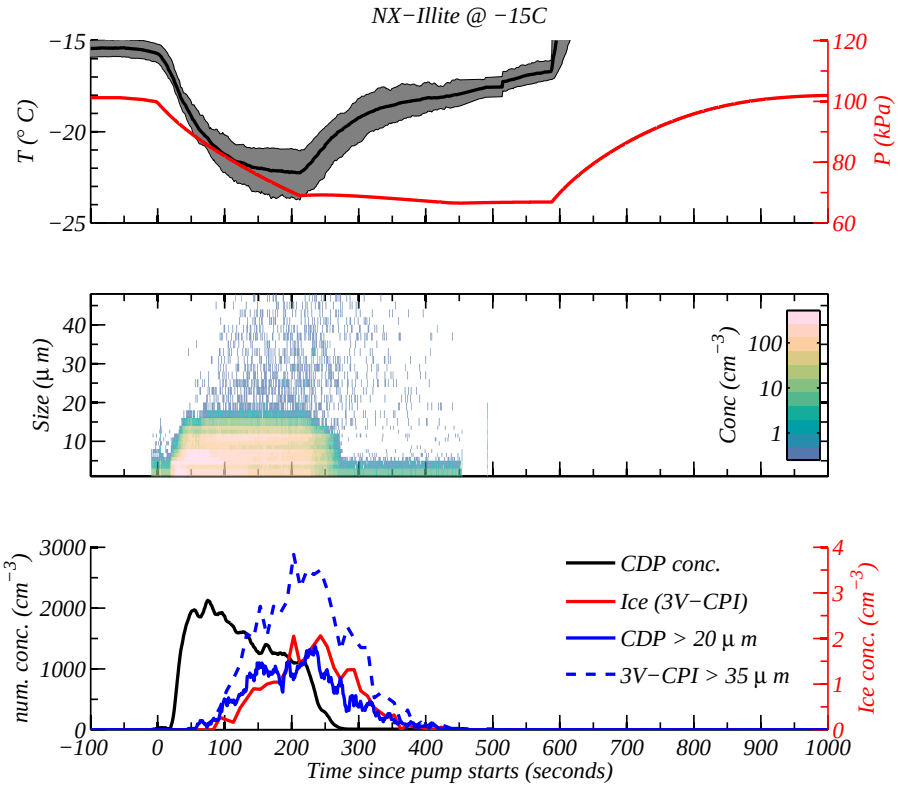

Figure 6. Same as Fig. 2, but for illite at −15 °C.

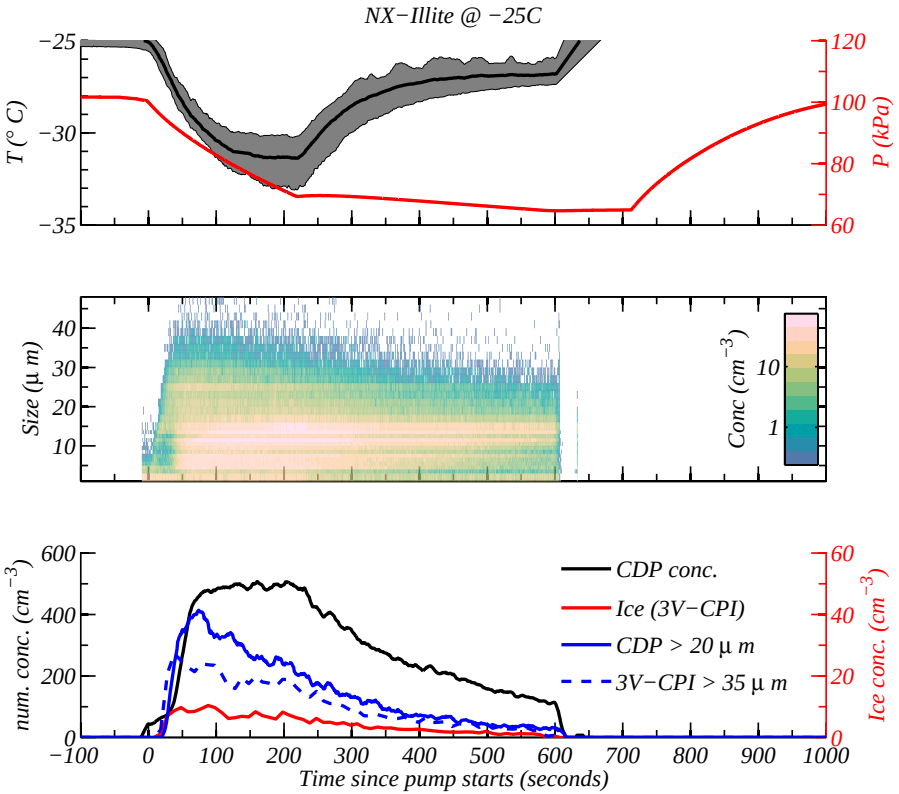

Figure 7. Same as Fig. 2, but for illite at −25 °C.

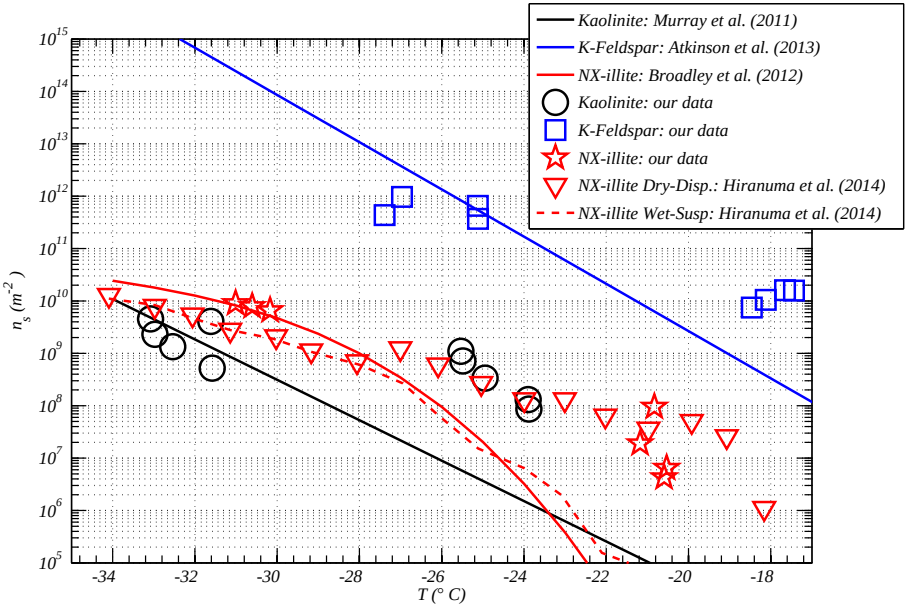

Figure 8. n_s values from the literature using wet-suspension methods are shown via the line plots: black line is for kaolinite from Murray et al. (2011); blue line is for K-feldspar from Atkinson et al. (2013); red solid line is for NX-illite from Broadley et al. (2012); red-dashed line is for NX-illite from Hiranuma et al. (2014). The open symbols correspond to n_s values derived using dry-dispersion: black circles are our data for Kaolinite; blue squares are our data for K-feldspar and stars are our data for NX-illite. Downward pointing triangles are for the NX-illite data derived using dry-dispersions from Hiranuma et al. (2014). For our data, measurement errors are typically the size of the symbols or less (see Table 1)

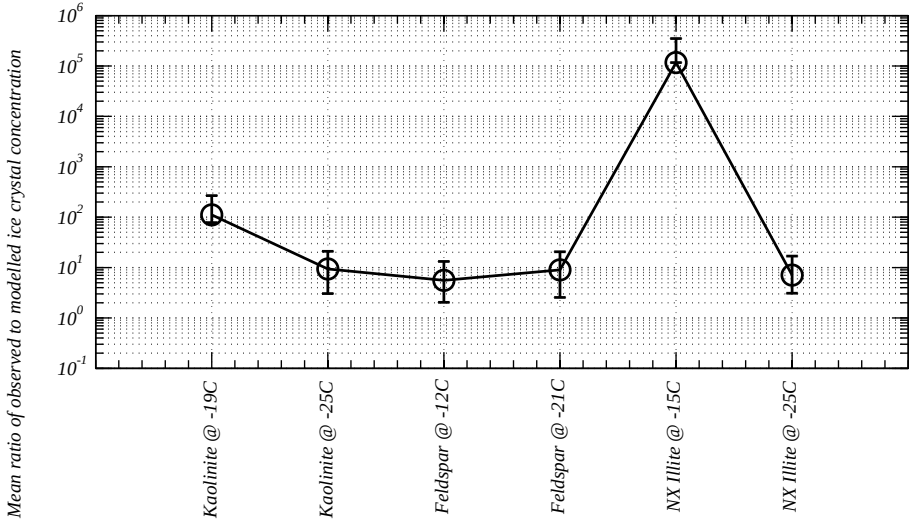

Figure 9. Figure summarising the results of the ACPIM simulations. The metric shown is the ratio of observed to modelled ice crystal number concentrations averaged over all expansions in a set of experiments. Error bars are 25th and 75th percentiles. The ACPIM model used the parametrisations from Murray et al. (2011); Broadley et al. (2012); Atkinson et al. (2013) for kaolinite, illite and K-feldspar particles respectively.

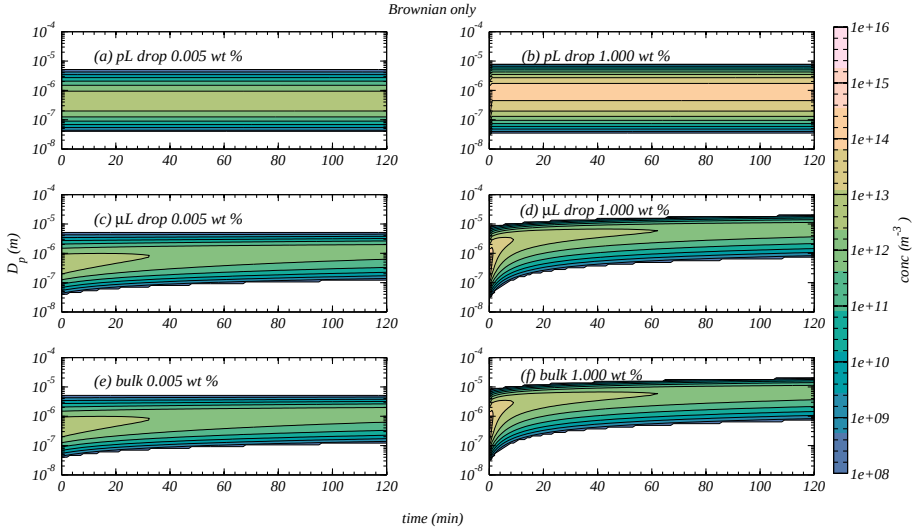

Figure 10. Numerical model simulations of the coagulation of mineral particles within suspension showing the size distribution evolution vs time. **(a)** is for a 0.005 wt % suspension inside a pico litre drop; **(b)** is the same as **(a)** but for 1.000 wt %; **(c)** is for a 0.005 wt % suspension inside a micro litre drop; **(d)** is the same as **(c)** but for 1.000 wt %; **(e)** and **(f)** are the same as **(c)** and **(d)** respectively, but for an infinite volume.

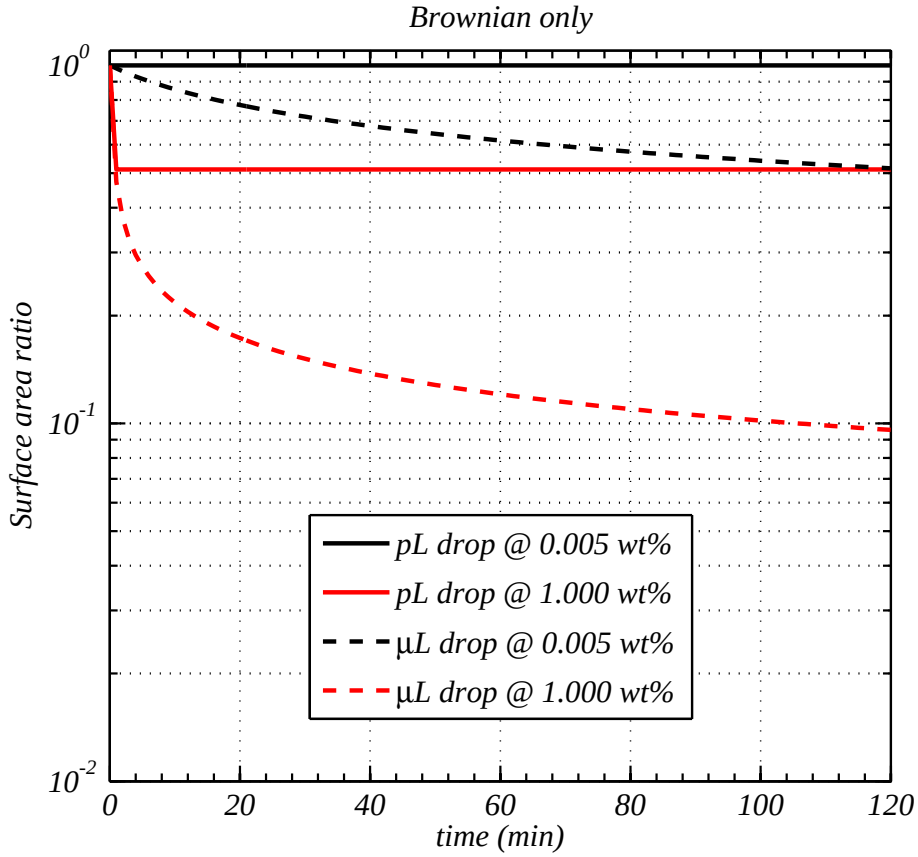

Figure 11. The evolution of the ratio of particle surface area to initial particle surface area for mineral particles undergoing coagulation in water suspension. The coagulation kernel assumed is that due to collisions arising from Brownian motion only.

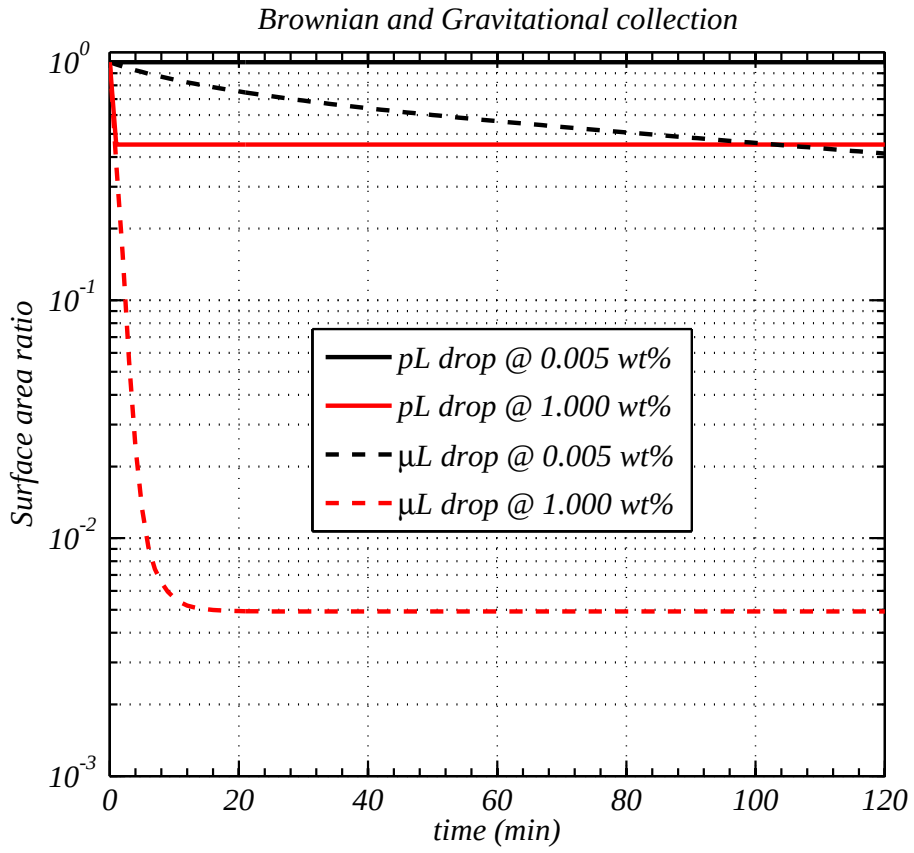

Figure 12. Same as Fig. 11, but with the coagulation due to Brownian motion and gravitational settling.

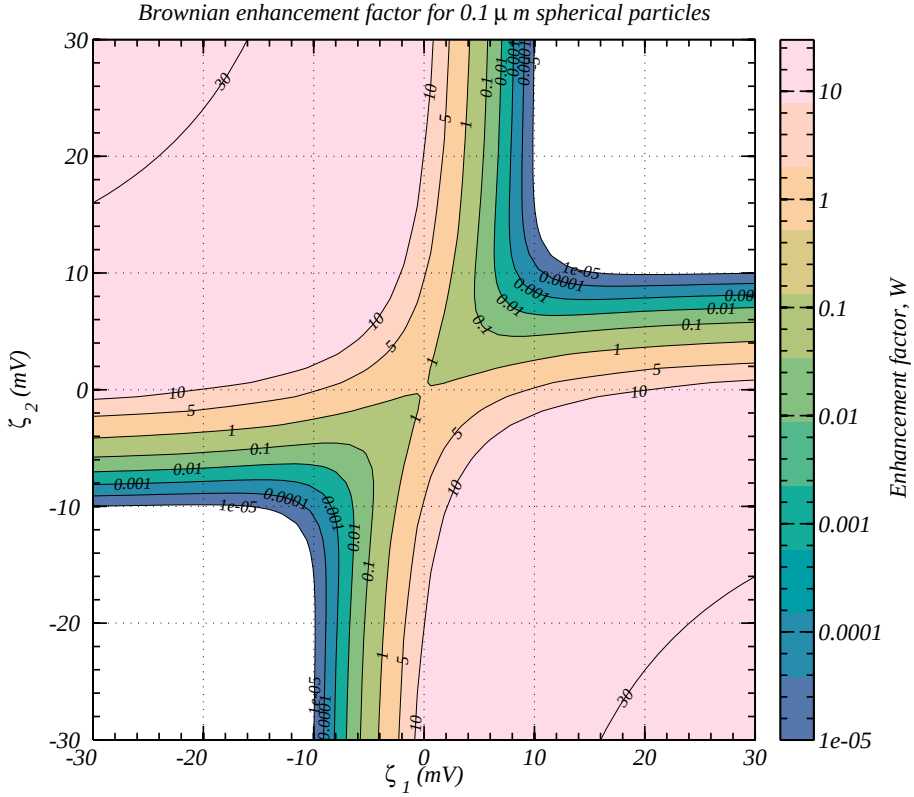

Figure 13. The enhancement factor of the Brownian collision kernel for two spherical particles in pure water as a function of the zeta-potential of both particles.